ACCEPTED FOR PUBLICATION IN THE ASTROPHYSICAL JOURNAL
Preprint typeset using LaTeX style emulateapj v. 04/03/99

THE EXTRAGALACTIC DISTANCE SCALE KEY PROJECT XXVII. A DERIVATION OF THE HUBBLE CONSTANT USING THE FUNDAMENTAL PLANE AND D_n-σ RELATIONS IN LEO I, VIRGO, AND FORNAX

DANIEL D. KELSON[1], GARTH D. ILLINGWORTH[2], JOHN L. TONRY[3], WENDY L. FREEDMAN[4], ROBERT C. KENNICUTT, JR.[5], JEREMY R. MOULD[6], JOHN A. GRAHAM[1], JOHN P. HUCHRA[7], LUCAS M. MACRI[7], BARRY F. MADORE[8], LAURA FERRARESE[9], BRAD K. GIBSON[10], SHOKO SAKAI[11], PETER B. STETSON[12], EDWARD A. AJHAR[11], JOHN P. BLAKESLEE[9], ALAN DRESSLER[4], HOLLAND C. FORD[13], SHAUN M.G. HUGHES[14], KIM M. SEBO[6], AND NANCY A. SILBERMANN[8]

Accepted for publication in the Astrophysical Journal

ABSTRACT

Using published photometry and spectroscopy, we construct the fundamental plane and D_n-σ relations in Leo I, Virgo and Fornax. The published Cepheid P-L relations to spirals in these clusters fixes the relation between angular size and metric distance for both the fundamental plane and D_n-σ relations. Using the locally calibrated fundamental plane, we infer distances to a sample of clusters with a mean redshift of $cz \approx 6000$ km s^{-1}, and derive a value of $H_0 = 78 \pm 5 \pm 9$ km s^{-1}Mpc^{-1} (random, systematic) for the local expansion rate. This value includes a correction for depth effects in the Cepheid distances to the nearby clusters, which decreased the deduced value of the expansion rate by $5\% \pm 5\%$. If one further adopts the metallicity correction to the Cepheid PL relation, as derived by the Key Project, the value of the Hubble constant would decrease by a further $6\% \pm 4\%$. These two sources of systematic error, when combined with a $\pm$6% error due to the uncertainty in the distance to the Large Magellanic Cloud, a $\pm$4% error due to uncertainties in the WFPC2 calibration, and several small sources of uncertainty in the fundamental plane analysis, combine to yield a total systematic uncertainty of $\pm$11%. We find that the values obtained using either the CMB, or a flow-field model, for the reference frame of the distant clusters, agree to within 1%. The D_n-σ relation also produces similar results, as expected from the correlated nature of the two scaling relations. A complete discussion of the sources of random and systematic error in this determination of the Hubble constant is also given, in order to facilitate comparison with the other secondary indicators being used by the Key Project.

Subject headings: Cepheids — galaxies: distances and redshifts — distance scale

1. INTRODUCTION

The goal of the distance scale Key Project is to measure distances to galaxies where the Hubble flow is expected to dominate over local velocity perturbations, and derive a value of the Hubble constant accurate to $\pm$10%. However, much of the controversy over the Hubble constant (H_0) arises from disagreements over the secondary distance indicators which are used (see, for example, Jacoby *et al.* 1992, Fukugita, Hogan, & Peebles 1993). Therefore, a concerted effort is required to define zero points for a variety of independent indicators, including, for example, the Tully-Fisher relation (Tully & Fisher 1977, Aaronson, Mould, & Huchra 1979), D_n-σ (Dressler *et al.* 1987, Lynden-Bell *et al.* 1987), surface brightness fluctuations (Tonry & Schneider 1988), and methods based on supernovae (cf. Riess, Press, & Kirshner 1996). By calibrating several distance indicators, understanding their systematic differences, and combining them in a sensible way, it is hoped that the stated goal of 10% accuracy may be achieved (Mould *et al.* 1999a).

In this paper, we use data from the literature to construct the fundamental plane (FP) and D_n-σ relations in Leo I, Virgo, and Fornax. A number of Cepheid distances have been published by the Key Project to Leo I, Virgo, and Fornax. These groups, or clusters have several early-type galaxies for which kinematic and photometric data exist in the literature. These data, with the Cepheid distances, allow us to calibrate the FP and D_n-σ relations, and thus use these relations as secondary distance indicators in the distance scale ladder. Using the fundamental plane and D_n-σ one can derive the distance to Coma and several other distant clusters, for which the peculiar velocities are expected

[1]Department of Terrestrial Magnetism, Carnegie Institution of Washington, 5241 Broad Branch Rd., NW, Washington, DC 20015
[2]University of California Observatories / Lick Observatory, Board of Studies in Astronomy and Astrophysics, University of California, Santa Cruz, CA 95064
[3]Inst. for Astronomy, 2680 Woodlawn Dr., Honolulu, HI 96822
[4]Carnegie Observatories, Pasadena CA 91101
[5]Steward Observatories, University of Arizona, Tucson AZ 85721
[6]Research School of Astronomy & Astrophysics, Institute of Advanced Studies, Australian National University, ACT 2611, Australia
[7]Harvard-Smithsonian Center for Astrophysics, Cambridge, MA 02138
[8]IPAC, California Institute of Technology, Pasadena CA 91125, USA
[9]Department of Astronomy, California Institute of Technology, Mail Stop 105-24, Pasadena CA 91125
[10]Center for Astrophysics & Space Astronomy, University of Colorado, Boulder CO 80309-0389
[11]National Optical Astronomical Observatory, Tucson, AZ 85726
[12]Dominion Astrophysical Observatory, Victoria, BC V8X 4M6, Canada
[13]John Hopkins University and Space Telescope Institute, Baltimore MD 21218
[14]Royal Greenwich Observatory, Cambridge CB3 0EZ, UK; Current address: Institute of Astronomy, Madingley Road, Cambridge, CB3 0HA, UK

to be a small component of the observed radial velocities, and accurately determine the local expansion rate.

The results of this work can be directly compared to Sakai *et al.* (1999) who calibrate the local Tully-Fisher relation (Tully & Fisher 1977), and use it to measure distances to clusters in the flow-field; Ferrarese *et al.* (1999), who calibrate other Population II indicators such as the planetary nebula luminosity function, and the surface brightness fluctuation method; and Gibson *et al.* (1999), who recalibrate the Type Ia supernovae method. The values of H_0 from each of these secondary indicators are combined with the results from the fundamental plane and D_n-σ by Mould *et al.* (1999a) and Freedman *et al.* (1999).

This paper is structured as follows. In §2, we give a brief introduction to the fundamental plane and D_n-σ scaling relations. Section 3 outlines the data taken from the literature, as well as the subsequent treatment required to ready the data for fundamental plane analysis. We discuss the Cepheid distances to Leo I, Virgo, and Fornax in §4. In §5 the fundamental plane relations in Leo I, Virgo, and Fornax are compared to that in Coma and in other distant clusters and a value for the Hubble constant is derived. Section 6 is devoted to the analysis of the local D_n-σ relation, with its implied value of the Hubble constant, and a comparison of the D_n-σ relation with the FP. Following a brief discussion of the scatter in the local fundamental plane and D_n-σ relations in §7, we discuss systematic corrections to the derived value of H_0 (§8). A final value for the Hubble constant is given in §9, along with a detailed error budget and an estimate of the total uncertainty. Lastly, a brief comparison of our data with previous work in the literature is presented in Section 10.

2. THE FUNDAMENTAL PLANE AND D_n-σ RELATIONS AS DISTANCE INDICATORS

Elliptical galaxies appear to be a family of objects described by a small number of physical parameters. Because of dynamical equilibrium and the virial theorem, one expects that the characteristic internal velocities of elliptical galaxies should be correlated with their binding energies, and assuming light traces mass in a similar way for all elliptical galaxies, one therefore predicts a correlation between σ, and luminosity. In this way, the Faber-Jackson relation of elliptical galaxies (Faber & Jackson 1976) is analogous to the Tully-Fisher relation for spirals: The Faber-Jackson relation allowed for early-type galaxies to be used as standard candles for measuring distances to massive clusters, measuring the Hubble constant, and mapping the peculiar velocity field.

The introduction of surface brightness by Dressler *et al.* (1987) was a major improvement to the Faber-Jackson relation, reducing the scatter in elliptical galaxy scaling relations by 50%. The D_n-σ relation blended the observables of galaxy size and surface brightness by defining D_n, the diameter within which the surface brightness was equal to some fixed value. For galaxies with similarly shaped growth curves, D_n is a well-defined function of half-light diameter, D_e, and mean surface brightness, $\langle I \rangle_e$, within D_e, such that $D_n = f(D_e, \langle I \rangle_e)$.

Simultaneously, Djorgovski & Davis (1987) reported a "fundamental" relation between r_e, σ, $\langle I \rangle_e$. Both groups speculated that D_n-σ was simply an edge-on projection of the new "fundamental plane:"

$$r_e \propto \sigma^{\alpha} \langle I \rangle_e^{\beta} \tag{1}$$

where $\alpha \approx 1.2$ and $\beta \approx -0.85$ (Djorgovski & Davis 1987). Lucey, Bower, & Ellis (1991) later reiterated the point, while noting that D_n-σ residuals were correlated with mean surface brightness. Subsequently, Jørgensen *et al.* (1993) used a sample of Coma cluster early-type galaxies to show that D_n-σ is a nearly edge-on, but imperfect projection of the fundamental plane relation.

More recently, Jørgensen *et al.* (1996) showed that the fundamental plane of early-type galaxies in Gunn *r* follows the relation

$$r_e \propto \sigma^{1.24} \langle I \rangle_e^{-0.82} \tag{2}$$

using 224 early-type galaxies in 11 clusters. Ellipticals and S0s appear to follow the same relation, both with very low scatter. In Coma, for example, the scatter is only 14% in r_e (*i.e.*, distance). In contrast to the Faber-Jackson relation which employed elliptical galaxies as a family of "standard candles," the tighter fundamental plane and D_n-σ scaling relations turn early-type galaxies into accurate "standard rods."

Given the homogeneity of early-type galaxy stellar populations (*e.g.*, Sandage & Visvanathan 1978, Bower, Lucey, & Ellis 1992) the existence of a plane follows from basic principles (Faber *et al.* 1987). While the details of the physical basis behind the empirical relation remain elusive (Pahre 1998; though see Kelson 1998), the general picture of early-type galaxies in dynamical equilibrium with fairly homogeneous stellar populations seems to provide a reasonable approximation to the observed fundamental plane (Kelson 1998, 1999).

With the assumption that early-type galaxies form a homologous family, the combination of the virial theorem and the fundamental plane implies that galaxy M/L ratios are strongly correlated with their structural parameters:

$$M/L \propto \sigma^{0.49} r_e^{0.22} \sim M^{1/4} \tag{3}$$

Thus, when the D_n-σ or fundamental plane relations are used as distance indicators, one makes several important assumptions: (1) M/L ratios scale with galaxy structural parameters in the same way, everywhere; and (2) early-type galaxies have similar stellar populations (age, etc.), for a given galaxy mass, everywhere.

While these assumptions may not necessarily be valid, they have been observationally verified by extensive work (Burstein *et al.* 1990, Jørgensen *et al.* 1996, though see Djorgovski *et al.* 1988). More recently, however, Gibbons, Fruchter, & Bothun (1998) have discovered evidence that the fundamental plane scatter is related to environment, such that clusters which are not X-ray luminous have poorly-defined fundamental planes. However, such departures from universality are relevant to the derivation of peculiar velocities, and are of limited concern for the determination of the mean expansion rate of the local universe. The chief requirement for our use of the fundamental plane as a secondary distance indicator is that the slope and scatter of the *mean* relation in the distant clusters be similar to the local, calibrating samples. While this is shown explicitly in Section 5, we have an *a priori* expectation that this assumption be valid for the following reasons: (1) the fundamental plane, as an empirical relation, is a combination of a systematic variation of stellar populations with galaxy mass with correlated observational errors and selection biases (Faber *et al.* 1987, Kelson 1998, 1999); (2) this systematic trend in the properties of the stellar populations is the same in Virgo and Coma (Bower *et al.* 1992); and (3) residuals from the fundamental plane relation for cluster E/S0s are uncorrelated with other stellar populations indicators (*e.g.*, Jørgensen *et al.* 1996, Kelson *et al.* 1999c).

Nevertheless, despite any uncertainties behind the origin and universality of the fundamental plane, its utility as a distance indicator has been empirically established, and consistently reaffirmed (*e.g.*, Jørgensen *et al.* 1996 and others). Since their inception, several groups and teams of people have successfully used the fundamental plane to measure distances to individual elliptical galaxies, and to groups and clusters, in efforts to derive values of the Hubble constant or map the local flow-field (*e.g.*, Dressler *et al.* 1987, Wegner *et al.* 1996, Hudson *et al.* 1997). Given the reliability with which this distance indicator can be used, we now attempt to use the database of published Cepheid distances to calibrate the fundamental plane, and derive a value for H_0.

3. THE DATA

In this section, we discuss the sources of data used in our analysis, derive structural parameters for a sample of early-type galaxies in Leo I, Virgo and Fornax, collect useful data from the literature, and discuss the typical uncertainties in our fundamental plane data. The galaxies in the sample are listed in Table 1.

The fundamental plane relies on two types of data: photometry and spectroscopy. Galaxy imaging data, or aperture photometry, must be of sufficiently high S/N to derive effective radii (θ_e, in angular units; and r_e, in metric units) and mean surface brightnesses within the effective radii. Furthermore, the photometric calibration must be consistent for each set of galaxies to be placed on the fundamental plane. Therefore, we choose to use the CCD photometry of Tonry *et al.* (1997). As for the spectroscopy, the S/N must be sufficient to measure internal kinematics from absorption line widths. Our adopted velocity dispersions come from several reliable sources, discussed below. Lastly, because our estimate of the Hubble constant relies on direct comparisons of data from different sources, considerable care was taken to measure the calibrators using the same procedures which were used in analyzing the distant samples.

3.1. *Velocity Dispersions*

The Virgo and Fornax galaxies we use in this analysis were taken from the Dressler *et al.* (1987), who reported velocity dispersions for 20 galaxies in Virgo and 8 in Fornax. These data were obtained as part of a B_T-limited survey of elliptical galaxies, and the spectroscopy for the Virgo and Fornax galaxies were obtained primarily at Las Campanas Observatory (LCO). These Virgo and Fornax data form our initial sample, but their numbers were subsequently reduced by two due to a lack of precision photometry.

For the early-type galaxies in Leo I, we use Faber *et al.* (1989) who report velocity dispersions for N3377 and N3379, corrected to an effective aperture at the distance of Coma. We supplemented these with central velocity dispersions for N3384 and N3412 taken from Fisher (1997).

Jørgensen *et al.* (1995a) tested the accuracy of the Dressler *et al.* (1987) dispersions. No significant systematic difference was found between the dispersions measured by Jørgensen *et al.* and those that Dressler *et al.* obtained at LCO. The scatter between their observations was ~7%, resulting in a random error in distance for an individual galaxy of ~9%. Given this, the Jørgensen *et al.* (1995a) collection of spectroscopic parameters could be homogenized and placed on a single consistent system in agreement with Dressler *et al.* (1987).

3.1.1. *Velocity Dispersion Aperture Corrections*

Early-type galaxies have radial gradients in velocity dispersion, σ, and radial velocity, V_r (*e.g.*, Davies 1981, Tonry 1983). The implication is that the σ one measures depends upon the metric aperture used to extract the original spectra. Typically, one's aperture is defined by an angular extent upon the sky, so the metric aperture which defines the velocity dispersion typically increases with distance to a given galaxy. This variation in aperture with distance can be a source of systematic error for the fundamental plane and must be accounted for when making distance determinations.

Early-type galaxies can be partially supported by rotation, and velocity dispersion measurements are mixture of both pressure and rotational support. The dependency of σ upon aperture is not straightforward to predict. The observation of a dispersion is akin to taking a luminosity-weighted mean of the second moment of the line-of-sight velocity distribution, $\sigma^2 + V_r^2$, within some predefined spectrograph aperture. This second moment is also weighted by the surface brightness distribution of the galaxy within the aperture. Thus, measurements of σ depends on each galaxy's intrinsic distribution of orbits, as well as its light distribution (*e.g.*, Tonry 1983).

We chose to use the aperture correction prescription of Jørgensen *et al.* (1995a). They used photometry and long-slit spectroscopy from the literature to construct dynamical models of early-type galaxies. These models were projected onto the sky, and "observed" in order to determine how the measured velocity dispersion depends upon aperture size. They found that the measured dispersions described a power law function of the aperture size, d,

$$\log\sigma_{\rm cor} = \log\sigma_{\rm obs} + 0.04 \times (\log D_{\rm cor} - \log D_{\rm obs}) \qquad (4)$$

where $D_{\rm cor}$ is the nominal aperture, and $D_{\rm obs}$ is the aperture of the observation. This prescription implicitly incorporates both the declining velocity dispersion profiles of early-type galaxies, and the rising rotation curve as well.

We can use Eq. 4 to correct the observed velocity dispersions of galaxies in Leo I, Virgo, and Fornax to equivalent measurements from a nominal aperture with a $3''.4$ diameter at the distance of Coma, the system used for the Jørgensen *et al.* (1996) sample. This aperture is equivalent to a diameter of $D \approx 31''$ at the distance of Leo I, ~$20''$ at the distance of Virgo, and ~$15''$ for Fornax. The Dressler *et al.* (1987) Virgo and Fornax measurements were obtained using apertures of $D = 16''$ so the aperture corrections for the Dressler *et al.* dispersions are small (–1% in Virgo, +1% in Fornax). The Fisher (1997) measurements for N3384 and N3412 were derived using an aperture of $4'' \times 2''$, equivalent to a circular aperture of $D = 3''.8$, and thus required an aperture correction of –8%. The Faber *et al.* (1989) data for N3377 and N3379 had been corrected for aperture, by –5%, but we removed their correction in order to apply the Jørgensen *et al.* (1995a) prescription's aperture correction of –9%.

3.2. *Photometric Structural Parameters*

In this section, we discuss the determination of the photometric parameters required for the analysis of the fundamental plane. In particular, we derive the effective radii and surface brightnesses for the galaxies in the three nearby clusters, and discuss the transformation of the photometry to Gunn r, the system used by Jørgensen *et al.* (1996) for the sample of distant clusters.

3.2.1. *Effective Radii and Mean Effective Surface Brightnesses*

Tonry *et al.* (1997) observed more than 150 galaxies as part of a program to measure surface brightness fluctuations (SBF) in a large sample of early-type galaxies and spiral bulges. These SBF measurements provide a direct estimate of the distance to each galaxy and these distances are being used to determine H_0 and map the nearby peculiar velocity field (*e.g.*, Tonry *et al.* 1997). Those authors used CCD imaging in two colors, Johnson V and Cousins I_c, from several cameras and telescopes, making a painstaking attempt to unify the calibrations in one homogeneous system. Multiple observations of each galaxy showed that the V-band CCD photometry has uncertainties of ± 0.02 mag, and the $V-I_c$ colors have uncertainties of ± 0.02 mag (see §9 for further discussion). These data prove to be ideal for fundamental plane analysis.

The Tonry *et al.* (1997) sample included circular aperture photometry on 18 Virgo and eight Fornax galaxies of the ones listed in Dressler *et al.* (1987), and four early-types in Leo I. Tonry *et al.* masked out bright stars, overlapping objects, saturated pixels, other image defects, and removed the sky background. The S/N is extremely high, with negligibly small formal errors. The concentric aperture photometry profiles in the V band are shown as thick solid lines in Figure 1.

These data are well-suited for the fitting of parameterized growth curves. For consistency with the Jørgensen *et al.* (1996) fundamental plane we fit integrated $r^{1/4}$-law profiles to the galaxy growth curves. The curves were iteratively fit to a limiting radius of 2-3 times r_e in an effort to minimize the effects of sky-subtraction errors in the fit. In Figure 1, we show the fitted integrated $r^{1/4}$-law by a thin solid line. Residuals from this fit are shown as well. The resulting V-band effective radii (θ_e, in arcsec) and $\langle I \rangle_e$ are listed in Table 1.

The typical uncertainty in the fitted θ_e is 9%. However, there are some galaxies for which the errors are as large as 20-30%. Because the errors in θ_e and $\langle I \rangle_e$ are strongly correlated (see §6, and, *e.g.*, Saglia *et al.* 1997, Kelson *et al.* 1999b), the uncertainties in the surface brightnesses show correspondingly large, correlated errors (with a correlation coefficient of –0.73; also see Kelson *et al.* 1999b). What is important to note, however, is that the error in the combination of θ_e and $\langle I \rangle_e$ that enters the fundamental plane ($\theta_e \langle I \rangle_e^{0.82}$, the fundamental plane parameter) will be much smaller than the errors in the individual structural parameters (typically on the order of $\pm 3\%$).

The tabulated errors in θ_e and $\langle \mu \rangle_e$ do not include systematic errors which are incurred by adopting a parameterized profile (the de Vaucouleurs profile). Therefore, we experimented with generalizing the surface brightness profiles to the Sersic (1966) $r^{1/n}$-law. By generalizing the growth curves we find a mean systematic offset of –1% in distance in the combination of θ_e and $\langle I \rangle_e$ that enters the fundamental plane. The 1-σ scatter about this mean offset is $\pm 5\%$. We conclude that any systematic effect due to galaxy profile shapes has no significant impact on our results. We are confident that no significant systematic errors are incurred by adopting the de Vaucouleurs $r^{1/4}$-law as the parameterization of the galaxy surface brightness profiles (see Kelson *et al.* 1999 for a more detailed discussion).

To summarize, we anticipate that the systematic errors in the fundamental plane parameters are $< 1\%$. The random errors dominate for a given galaxy and are $\pm 5\%$ in distance. These uncertainties do not include, for example, the systematic errors of the photometric calibration, which will be discussed later.

3.2.2. *Transformation to Gunn r Photometry*

The Jørgensen *et al.* (1996) sample of 224 early-type galaxies in 11 nearby clusters was based on a compilation of photometry in Gunn r (Jørgensen *et al.* 1995b). Thus, in order to directly compare the fundamental plane relations in Leo I, Virgo, and Fornax with the fundamental plane relations of Jørgensen *et al.*, we need to transform our V-band surface brightnesses to r. We employ the photometric transformation of Jørgensen (1994), who used 75 photometric standards to derive the following transformation between V, $(B-V)$ to Gunn r:

$$r = V + 0.273 - 0.486(B-V) \qquad (5)$$

The Tonry *et al.* (1997) photometry is in V and I_c, so we used Frei & Gunn *et al.* (1994) to derive $(B-V) \approx 0.814 \times (V-I_c)$. Before applying the transformation, the Galactic foreground extinctions for each galaxy are individually removed. The extinction estimates, given in Table 1, were derived from Schlegel *et al.* (1998). The reddening law of Cardelli, Clayton & Mathis (1989) was used to calculate the extinctions in the V and I_c passbands.

Small corrections due to $(1+z)^4$ surface brightness dimming, and small K-corrections were applied to the Tonry *et al.* (1997) photometry as well. In Gunn r, the K-correction is well described by $2.5\log(1+z)$ (Jørgensen *et al.* 1995b). The published Jørgensen *et al.* data were already corrected for these effects.

We defer discussion of the errors in photometry and photometric transformation to Section 9.

3.2.3. *Derivation of r_n in the Gunn r Passband*

The fundamental plane and D_n-σ relations are closely related (Faber *et al.* 1987, Jørgensen *et al.* 1993), and so we derive the isophotal radii of the Leo I, Virgo, and Fornax galaxies to facilitate comparison of the two distance indicators. Similar to the effective radii derived earlier, we define θ_n to be the angular radius within which each galaxy has a specific mean surface brightness, and r_n is the equivalent radius expressed in metric units.

Using the transformation of Equation 5, and the mean $(V-I_c)$ colors of the galaxies, we transformed the concentric circular photometry to Gunn r in order to derive isophotal radii $\theta_n \equiv D_n/2$ in the same filter as was used to derive θ_n for the Coma galaxies. Jørgensen *et al.* (1995b) defined θ_n in Gunn r as the radius within which the mean surface brightness is 19.6 mag/arcsec^2. The values of θ_n are also listed in Table 1.

Our measurements of θ_n should be as well-determined as the fundamental plane parameters (see previous discussion). Errors in θ_n come from uncertainties in the transformation to Gunn r, the calibration of the original V photometry, uncertainties in the color gradients, photon statistics, and the noise characteristics of the detector. Because the color gradients in these galaxies are typically small ($|d(V-I_c)/d\log\theta| \lesssim 0.05$ mag/dex), we do not expect them to significant affect the r_n measurements (also see §9.3.4). For the moment, we assume that the errors in θ_n are similar to the errors in $\theta_e \langle I \rangle_e^{0.82}$.

4. THE CEPHEID DISTANCES TO LEO I, VIRGO, AND FORNAX

Cepheids remain a key component of the distance scale ladder for individual galaxies, and hence for the calibration of such secondary distance indicators. One assumption in our analysis is that the Cepheid distances to the spiral galaxies in these clusters/groups are appropriate for the early-types which we have

also associated with those clusters/groups. A good estimate for the error incurred by this assumption is not easy to determine, but the low scatter among the Cepheid distances to Virgo may indicate that this error is small. This uncertainty is one of many sources of error to be discussed in the discussion of the error budget in §9. The published Cepheid distances to the spiral galaxies in the Leo I group and the Virgo and Fornax clusters are listed in Table 2, along with their references (see Ferrarese *et al.* 1999). In deriving a weighted mean distance to Virgo, we exclude NGC 4639.

Our adopted distance mean moduli to Leo I, Virgo, and Fornax, weighted by the random errors, are $30.08 \pm 0.11 \pm 0.16$ mag, $31.03 \pm 0.04 \pm 0.16$ mag, and $31.60 \pm 0.14 \pm 0.16$ mag, respectively. These distance moduli correspond to metric distances of $10.4 \pm 0.6 \pm 0.8$ Mpc, $16.1 \pm 0.3 \pm 1.2$ Mpc, and $20.9 \pm 1.4 \pm 1.6$ Mpc. These distances are tied to the LMC distance modulus, where we have adopted $\mu_{\rm LMC} = 18.50 \pm 0.13$ mag.

The uncertainties in our distances to Leo I, Virgo, and Fornax are the systematic and random errors, respectively, arising from the Cepheid distance estimates alone. For the total random uncertainties, we have added the random errors in the individual Cepheid distances in quadrature with the standard error of the mean distance. The various sources of error in the Cepheid distances are listed in Table 3. Some of these components are exacerbated by the de-reddening procedure, such as the uncorrelated errors in the F555W and F814W photometric zero points (which systematically impacts H_0), or the errors in the F555W and F814W aperture corrections (which is a random error for each Cepheid-based distance). Thus, the systematic errors given in the previous paragraph are simply a combination of uncertainty in the distance to the LMC, the uncertainties in the LMC PL relations themselves, and the uncertainties in the WFPC2 photometric calibration. The estimates for the random errors to each cluster are assumed to be comparable to the random error to a given galaxy, divided by root-N.

After some of these distances were published, Kennicutt *et al.* (1998) measured a marginally significant dependence of the Cepheid PL relation on metallicity of $\Delta\mu_{VI_c} = -0.24 \pm 0.16$ mag per dex in [O/H]. Differences between the abundances in our Cepheid fields and the LMC lead to systematic errors in the inferred distances. For some secondary indicators, the Cepheid calibrating fields span a wide range of oxygen abundances with a mean abundance equal to that in the LMC. Such is the case for the Tully-Fisher relation, for which the effects of metallicity incur a net effect on the Hubble constant of zero (Sakai *et al.* 1999). In this paper, the number of Cepheid calibrators is small, with a mean metallicity greater than that in the LMC. Thus metallicity corrections to the PL relation will have a systematic effect on H_0 and this systematic effect will be discussed in §8.

5. THE FUNDAMENTAL PLANE AND A DETERMINATION OF THE HUBBLE CONSTANT

5.1. *The Fundamental Plane Relations of Leo I, Virgo, and Fornax*

The fundamental plane in the three clusters is shown in Figure 2(a). For our analysis, we convert the surface brightnesses to units of $L_\odot/{\rm pc}^2$ in the bandpass of interest (Gunn r), and refer to the effective radii by r_e, in metric units of kpc, using the Cepheid distances to each cluster or group adopted in the previous section.

Fixing the slope of the fundamental plane to that found in the distant cluster sample by Jørgensen *et al.* (1996), the zero point is defined as $\gamma \equiv \log r_e - 1.24 \log\sigma + 0.82 \log\langle I\rangle_e$. In Jørgensen *et al.* (1996), the sample sizes were large, and as a result, those authors defined the zero points using the median, a technique that is robust to outliers. However, because our samples in Leo I, Virgo and Fornax are so small, we opt for the mean zero point, rather than the median, even though using the median does not lead to significantly different results.

Because the values of r_e for the Leo I, Virgo, and Fornax galaxies have all been expressed in metric units, the galaxies should all lie along the same line in the figure. Any scatter in the figure from galaxy to galaxy, or from cluster to cluster should only arise from (1) an error in Cepheid distance; (2) a breakdown in the assumption that that Cepheid distance applies to the early-types in the group or cluster; (3) errors in the fundamental plane parameters themselves; or (4) inhomogeneities in galaxy M/L ratio from galaxy to galaxy. These potential sources of error will be discussed below in §9, but they are clearly not large given that the three cluster samples agree so well in the figure.

Before deriving the fundamental plane zero point, we note that the CCD imaging of N4552 was saturated in the core. Thus, its derived mean surface brightness is in error, and we exclude it from subsequent analysis. Furthermore, N4489 is 0.09 mag bluer (3σ) than the mean $(V-I_c)$ color of the other early-type galaxies and is also excluded. Lastly, Tonry *et al.* (1997), using SBF measurements, argue that N4365 and N4660 are not *bona fide* members of Virgo. As a result of removing these objects, our final sample is comprised of 4 galaxies in Leo I, 14 in Virgo, and 8 in Fornax, as shown in the plot of the calibrated fundamental plane in Figure 2(a).

In Table 4, we give mean fundamental plane zero points, $\langle\gamma\rangle$, derived in each cluster and their formal errors. The external systematic and random errors are shown in the last column. Given the magnitude of the internal and external random errors, the zero points in the three clusters agree remarkably well. Taking a weighted average of the three gives $\langle\langle\gamma\rangle\rangle = -0.173 \pm 0.013$. By computing the mean zero point using all 26 galaxies at once, instead of averaging the individual zero points of the clusters, one finds no significant change in the mean fundamental plane zero point, $\langle\langle\gamma\rangle\rangle$. This error is the quadrature sum of the standard error of the mean and the random errors in the Cepheid distances to the clusters. The scatter among the three cluster zero points is consistent with the uncertainties in the individual zero points and the random errors in the Cepheid distances, suggesting that the intrinsic differences in the mean galaxy M/L ratios among the three clusters are not large. None of the individual cluster zero points differ from the mean by more than 1.5σ, when one takes into consideration the internal errors, and the random errors in the Cepheid distances. The full error budget will be discussed below in §9.

This reported zero point is only valid for the set of fundamental plane slopes adopted above. Changing α and β will produce different zero points in both the calibrating and distant samples, leading to small changes in the derived relative distance. We will explore this source of uncertainty in §9.

5.2. *The Fundamental Plane in Distant Clusters and the Hubble Constant*

The fundamental plane zero point explicitly relates angular size of θ_e to a metric scale. By comparing the zero point of the metric ($\log r_e$) fundamental plane to the angular ($\log\theta_e$) funda-

mental plane in a distant cluster, one directly infers its distance.

For example, Jørgensen *et al.* (1995ab) provide fundamental plane data for 81 galaxies in Coma. Using θ_e in radians, one finds a zero point for Coma of $\gamma_C = -5.129 \pm 0.009$. Thus the distance to Coma, in Mpc can be written as $\log d = 5.129 + \langle\gamma\rangle - 3$. (The additional constant converts the distances to units of Mpc.) Using the weighted mean zero point defined in the previous section, one derives a distance to Coma of 90 ± 6 Mpc. Correcting for this distance, we show the galaxies in the Coma sample in Figure 2(a) as small points. Note that the nearby galaxies follow the same relation as that in Coma, validating our assumption that the distant fundamental plane be of the same shape and scatter as that in the nearby clusters. Using a recession velocity for Coma of 7143 km s^{-1}, one obtains $H_0 = 79 \pm 6$ km s^{-1}Mpc^{-1}. These include only the random errors, all of which are discussed with the total error budget in §9.

Distant clusters can have peculiar velocities, which may lead one to deduce incorrect values for the Hubble constant. Therefore, we choose to derive a mean value of the Hubble constant using several distant clusters, with the hope that errors in individual measurements due to the peculiar velocity field will be reduced (see below), by $\sqrt{N}$. For this paper, we use the 11 distant clusters of Jørgensen *et al.* (1996).

In Table 5, we list all 11 clusters, the number of galaxies used in each of them, the fundamental plane zero points for each cluster (again, using θ_e in radians), the *rms* scatter, the implied distance to each cluster, the recession velocity of each cluster with respect to the cosmic microwave background (CMB) and the implied Hubble constant, and the recession velocity of each cluster with respect to the flow-field model of Mould *et al.* (1999a) and the implied Hubble constant. The errors which are listed are the quadrature sum of the random errors in the Cepheid-based zero point, the random errors in the zero points of each cluster, and the random errors due to uncertainties in the fundamental plane slope (see §9.5).

The average value of H_0, weighting by the internal errors, over all 11 clusters is $\langle H_0\rangle = 82 \pm 5$ km s^{-1}Mpc^{-1}. This value is produced whether we use the CMB or flow-field recession velocities. Several of the distant clusters have poorly defined fundamental plane zero points. The largest individual zero point uncertainty is in Grm 15, for which the median zero point leads to a 15% larger value for H_0. Averaging over the 11 clusters and using the median zero points leads to a net increase of 3% in the Hubble constant. When using the five clusters with samples of $N \geq 20$ galaxies, we find a 2.5% decrease in the Hubble constant. We conclude that our results are insensitive to the distant cluster sample sizes.

For the five clusters with good statistics ($N \geq 20$ galaxies), the weighted *rms* scatter in the individual values of H_0 is 4%. We interpret this scatter as the uncertainty due to the peculiar velocity field when using a single distant cluster and incorporate this uncertainty into the error budget. Averaged over the 11 clusters, the resulting uncertainty in the Hubble constant due to the peculiar velocity field is expected to be 1%. To help test the effect of the velocity field, we computed H_0 using the six clusters with $cz_{\rm CMB} \geq 5000$ km s^{-1}, and the four clusters beyond $cz_{\rm CMB} \geq 7000$ km s^{-1}. A net difference of 1% in H_0 is observed. While the peculiar velocities for the distant clusters do contribute small random errors, we conclude that they are not a dominant source of our uncertainties in H_0. If one uses the flow-field velocities of Mould *et al.* (1999a), the results differ by no more than 1%.

The errors in the values of H_0 given above are the quadrature sum of the random error in the Cepheid-based zero point, the formal errors in individual zero points of the distant clusters, the random errors due to the uncertainties in FP slopes, and the error in the unknown peculiar velocity field.

Before correcting the value of H_0 for systematic effects, we now discuss a determination of H_0 using the D_n-σ relation. Following the analysis, we discuss D_n-σ in the context of the fundamental plane, and show why the value of the Hubble constant derived using the fundamental plane is to be preferred.

6. THE D_n-σ RELATION

The D_n-σ relation has traditionally been thought of as equivalent to the fundamental plane (Faber *et al.* 1987 and Djorgovski & Davis 1987). However, Jørgensen *et al.* (1993) argued that the two relations are not equivalent, that D_n-σ is not quite identical to the edge-on projection of the fundamental plane. Nevertheless, the D_n-σ relation can provide an additional test of the robustness of our results and illuminate our sensitivity to the systematic differences between the two scaling relations.

6.1. *The D_n-σ Relations of Leo I, Virgo, and Fornax*

In parallel with the fundamental plane analysis, though using the isophotal radii, r_n, derived in §3.2.3, we define the D_n-σ zero points as $\delta \equiv \log r_n - 1.24 \log \sigma$, much like the fundamental plane zero points were defined above. In Figure 2(b), we plot the D_n-σ relations of Leo I, Virgo, and Fornax. For this figure, the r_n values are expressed in kpc.

In Table 4, we list the values of $\langle\delta\rangle$ for each group/cluster. The D_n-σ zero points also agree remarkably well with each other, which should not be surprising given the intimate connection between D_n-σ and the fundamental plane. A weighted mean gives a value of $\langle\langle\delta\rangle\rangle = -2.395 \pm 0.013$. This error is the quadrature sum of the standard error of the mean and the random errors in the Cepheid distances to the clusters.

6.2. *The D_n-σ Relation in Distant Clusters*

We can now compare this calibrated D_n-σ zero point with the D_n-σ relations of the clusters in Jørgensen *et al.* (1996) to measure their distances, and thus derive a value of the Hubble constant for comparison with the one given previously in §5.

The results for each cluster are given in Table 5. For example, the 81 galaxies in Coma have a mean D_n-σ zero point of $\delta_C = -7.373 \pm 0.009$, in which θ_n is expressed in radians, Thus the distance to Coma, in Mpc can be written as $\log d = 7.373 + \langle\delta\rangle - 3$. Using the weighted mean of the Leo I, Virgo, and Fornax zero points, one derives a distance to Coma of 95 ± 7 Mpc. The D_n-σ relation for Coma is shown in Figure 2(b) by the small points. The implied value of the Hubble constant is $H_0 = 75 \pm 5$ km s^{-1}Mpc^{-1}. These errors, too, are the quadrature sum of the random errors.

Averaging over the 11 clusters, one finds $\langle H_0\rangle = 79 \pm 6$ km s^{-1}Mpc^{-1}, a difference of only 4% compared to the value found using the fundamental plane.

6.3. *The Relation between D_n-σ and the Fundamental Plane*

The assumption that the two relations are equivalent implies that $r_n \equiv r_e \langle I\rangle_e^{0.82}$. Using the Tonry *et al.* (1997) photometry we can investigate at what point this assumption breaks down. Dressler *et al.* (1987) showed that for a set of galaxies with identical growth curves, the ratio of r_n/r_e is indeed a power-

law function of $\langle I \rangle_e$ (without specifying the exponent). By fitting a universal growth curve to any set of galaxies with a range of profile shapes, the exponent is indeed constant, and furthermore is only a function of the what growth curve is used in the fitting (Kelson *et al.* 1999b).

We therefore performed a simple test to determine the relationship between r_n, r_e and $\langle I \rangle_e$. For the four Leo I galaxies, the 14 Virgo galaxies and the eight Fornax galaxies, plus the Jørgensen *et al.* (1996) sample of 81 Coma galaxies, we find

$$\log(r_n/r_e) = (0.73 \pm 0.01) \times \log[\langle I \rangle_e / \langle I \rangle_{r_n}] \qquad (6)$$

with a scatter of about 0.01 dex. This relation holds in each of the four clusters, as shown in Figure 3. The solid line, with the slope of unity in this projection, represents the above relation.

The above expression relates r_n to effective radius and mean surface brightness and explicitly shows that the D_n-σ scaling relation has a different shape from the fundamental plane. The D_n-σ relation can be thought of as a view of the fundamental plane which has been skewed by the correlated errors between r_e and $\langle I \rangle_e$. Thus we have confirmed the result of Jørgensen *et al.* (1993), who concluded that D_n-σ is a slightly curved projection of the fundamental plane.

The curvature of this projection is expected from the fact that the surface brightness profiles of early-type galaxies, in general, are well-described by $r^{1/4}$-laws. In Figure 3, the dashed line shows the relation between radius and mean surface brightness within that radius for an $r^{1/4}$-law. The curve is not a fit to the data but is simply a projection of the $r^{1/4}$-law growth curve. The conclusion is that r_n is not a linear approximation to the fundamental plane parameter, and that the accuracy of D_n-σ as a distance indicator is related to the range of galaxy sizes used in the scaling relation.

Both D_n-σ and the fundamental plane are affected by the correlation of error in r_e and $\langle I \rangle_e$. For the fundamental plane, galaxy scale lengths are difficult to measure to an accuracy of better than 50% (Caon *et al.* 1993, Kelson *et al.* 1999b). Monte Carlo simulations of the fundamental plane indicate that such large errors in half-light radii do not increase the scatter in the fundamental plane because the underlying scaling relation is reasonably parallel to the error correlation vector (within $\lesssim 15°$, Kelson 1999). In other words, large errors in r_e do not necessarily contribute to large errors in distance. In the case of the fundamental plane, the coefficient on the surface brightness term is not equal to $\beta = -0.73$, as it is implicitly in D_n-σ. Therefore, we conclude that the FP is likely to be less-biased by the error correlation, and will be a more reliable distance indicator.

7. THE SCATTER IN THE FUNDAMENTAL PLANE AND D_n-σ RELATIONS

The observed scatter in the Virgo fundamental plane and D_n-σ relations is very low; the 1-σ width is ± 0.045 dex in distance, implying a $\pm 10\%$ uncertainty in the distance to any individual galaxy. This low scatter is remarkable given that the uncertainties in the velocity dispersion have been estimated at $\pm 9\%$ for a single galaxy, and that the errors on our fundamental plane parameters are probably no larger than $\pm 5\%$. Furthermore, the Virgo galaxies have spatial extent on the sky, and there must be some corresponding depth to the sample. Our sample has an approximate *rms* scatter on the sky equivalent to 3°, which, for a spherical distribution, implies an additional $\pm 5\%$ scatter in distance along the line of sight. There is very little room left for other sources of scatter and it is likely that the estimates on the uncertainties of σ and $r_e \langle I \rangle_e^{-0.82}$ have been overestimated. With all of these sources of scatter, we conclude that the intrinsic scatter in the fundamental plane of Virgo must be very low, indicating remarkable homogeneity among their stellar populations.

If environment does play a key role in determining galactic M/L ratios, then the fundamental plane ellipticals in Virgo must be very similar indeed to the inner regions of Coma, where the observed scatter is also extremely low ($\pm 14\%$ in distance for a single galaxy).

The 1-σ scatter in the Fornax sample, is ± 0.092 dex, equivalent to 21% in distance (also seen by D'Onofrio *et al.* 1997). There is no obvious reason for this increase. The Fornax galaxies do not display any obvious morphological peculiarities, nor are their internal kinematics significantly different from normal ellipticals (Bender, Saglia, & Gerhard 1994). NGC 1344 has the largest residual and by excluding it from the zero point determination, the remaining seven show a scatter of ± 0.060 dex. This scatter implies that these Fornax ellipticals have an extra 10%, in distance, added in quadrature with the Virgo scatter, which would suggest (1) that the cluster is quite elongated along the line of sight; or (2) that the remaining seven early-type galaxies have slightly more scatter in their stellar populations. However, there is no obvious *a priori* reason to exclude NGC 1344 from the analysis, and doing so leads to no significant change in the Hubble constant, given the weight of the other seven galaxies in the cluster, and the weight that the Fornax zero point is given compared to Virgo or Leo I.

Given the range of Cepheid distances (0.4 mag), perhaps the ellipticals span a large range as well; however, assuming the same internal errors in the Virgo and Fornax data, the Fornax plane apparently has an additional 18% scatter added in quadrature. Only if Fornax is the chance superposition of two groups of ellipticals (near, with N1326A and N1365, and far, with N1425), can this be achieved. There is no strong evidence for this, but it is consistent with the suggestion by Suntzeff *et al.* (1999) that the hosts of the Type Ia supernovae in the direction of Fornax may be lying at a distance of 21.6 Mpc.

While the increased scatter in Fornax leaves open questions about the uniformity of early-type stellar populations and the intrinsic spread in the distances to Fornax ellipticals, we note that these uncertainties have a small impact on our value of the Hubble constant, because we use Leo I and Virgo as well, with Virgo having the highest weight. The increased weight that has been given to Virgo has its own implications, and we discuss those further below, in §8.3.

In the following sections we address the systematic corrections to the derived value of H_0, and potential sources of error in the current analysis.

8. SYSTEMATIC CORRECTIONS TO THE HUBBLE CONSTANT

In this section we discuss three potential sources of systematic error, and the corrections we make to our determination of H_0 for these systematic effects. The first systematic correction is due to the uncertain metallicity correction to the Cepheid P-L relation. Next, the cluster population incompleteness bias is discussed in the context of the fundamental plane samples. Lastly, we address the systematic correction to H_0 which arises by adopting distances to Leo I, Virgo, and Fornax which are derived from Cepheid distances to spirals selected from an extended distribution along the line-of-sight.

8.1. *The Metallicity Correction to the Cepheid Distances*

Kennicutt *et al.* (1998) found that the Cepheid P-L relation has a small dependence upon [O/H] abundance, such that two-color VI_c distance determinations are in error by $\Delta\mu_{VI_c}$ = -0.24 ± 0.16 mag/dex. The trend is such that metal-rich Cepheids appear brighter and closer than metal-poor ones. Because this determination is not very significant, it has not been factored into our determination of H_0.

Nevertheless, the uncertain metallicity correction is a source of systematic error, and we now estimate to what extent our adopted distances to Leo I, Virgo, and Fornax, are affected. The metallicity corrected distance moduli increase 8%, 6% and 4% for Leo I, Virgo, and Fornax, respectively, to $30.27 \pm 0.11 \pm 0.16$ mag, $31.17 \pm 0.05 \pm 0.16$ mag, $31.68 \pm 0.16 \pm 0.16$ mag. These correspond to metric distances of $11.3 \pm 0.6 \pm 0.9$ Mpc, $17.1 \pm 0.4 \pm 1.3$ Mpc, and $21.7 \pm 1.7 \pm 1.7$ Mpc, respectively.

Correcting for metallicity increases all of the adopted distances, and thus leads to a decrease in H_0. Using the metallicity correction derived by Kennicutt *et al.* (1998) leads to a value of $H_0 = 77 \pm 5$ km s^{-1}Mpc^{-1}. Therefore, if one were to use of the Kennicutt *et al.* metallicity correction would decrease the Hubble constant by $6\% \pm 4\%$.

8.2. *Cluster Incompleteness Bias*

The "cluster population incompleteness bias" (*e.g.,* Federspiel *et al.* 1994) occurs because one is attempting to measure the distance to standard candles in a magnitude-limited sample. One can simulate the magnitude of the bias by sub-sampling the Coma galaxies. We randomly select subsets of the Coma sample, imposing selection criteria in r_e, or in apparent magnitude, such that the randomly selected subset of the Coma data has the same size and depth as the samples in each of the 11 clusters. By performing 500 iterations of this selection for each cluster, we can estimate the systematic biases in the individual cluster zero points. In doing these Monte Carlo experiments, we find that the systematic bias is less than 1%.

The effect can be tested using the data as well, but the results are inconclusive because of small number statistics in most of the clusters. Jørgensen *et al.* (1996) showed that their samples are reasonably complete down to $\sigma > 100$ km s^{-1}. By including only those galaxies in the distant clusters with $\sigma > 100$ km s^{-1}, the mean Hubble constant, found by minimizing the square of the residuals in each of the clusters, decreases by 2%. Using a cut of $\sigma > 150$ km s^{-1}, the value decreases by less than 4%. However, we caution against adopting such a correction because it does not appear to be statistically significant. If we define the fundamental plane zero points of the distant clusters by minimizing the absolute residuals, the derived value of H_0 decreases by less than 1%, consistent with the Monte Carlo simulations of the previous paragraph.

This robustness of our result is also illustrated using the cluster with the largest sample, Coma, and varying the cut in velocity dispersion. When we use the mean zero point of the Coma fundamental plane, with no velocity dispersion cut, we obtain $H_0 = 82 \pm 6$km s^{-1}Mpc^{-1} (random). Using only those galaxies with $\sigma > 150$ km s^{-1}, and $\sigma > 200$ km s^{-1}, one obtains $H_0 = 80 \pm 6$ km s^{-1}Mpc^{-1}, and $H_0 = 81 \pm 6$ km s^{-1}Mpc^{-1}, respectively. When we minimize the absolute residuals in determining the fundamental plane zero point of Coma, we find $H_0 = 81 \pm 6$ km s^{-1}Mpc^{-1}, using only those galaxies with either $\sigma > 150$ km s^{-1}or $\sigma > 200$ km s^{-1}. This test is consistent with the Monte Carlo simulations, in which the magnitude of the bias is smaller than 1%.

Based on these tests we argue that the cluster population incompleteness bias is not a statistically significant systematic effect in our analysis of the Jørgensen *et al.* (1996) data.

We also test the magnitude of the bias in the calibrators by imposing similar cuts on velocity dispersion, in Leo I, Virgo, and Fornax. The net effect on the inferred value for H_0 is $\pm 1\%$. Using the $\sigma > 150$ km s^{-1}cut, H_0 decreases by 1%. For a cut of $\sigma > 200$ km s^{-1}, H_0 increases by 1%.

Thus, using the experiments listed above with all 11 clusters, with Coma alone, and with the nearby sample, we estimate that the cluster population incompleteness bias introduces an uncertainty of at most $\pm 2\%$.

8.3. *The Spatial Coincidence of the Spirals and Ellipticals*

Up until now, we have assumed that the early-type galaxies are co-spatial with spirals for which we have Cepheid distances. If this assumption is correct, there may still be depth effects in the three groups/clusters. For extended clusters like Virgo, there is an increased probability that galaxy targets are systematically selected from the near side of a given cluster, while the ellipticals are selected from the cluster core. Gonzalez & Faber (1997) modeled the effects of this bias for the Virgo cluster, and argued that the Key Project distance to Virgo may be under-estimated by 5-8% when using the Cepheid distance to M100 alone.

In this paper we now have 11 Cepheid distances to 3 clusters whose distances are uncertain to 2–7%, compared to the original $\pm 10\%$ distance to M100. The situation has clearly improved, but the potential for bias is still there. We have therefore carried out simulations of the type done by Gonzalez & Faber in order to quantify the bias. Now that we have 11 Cepheid distances, we can characterize the distance dispersion in the clusters, averaging over the three of them after appropriate scaling. This is appropriate, as there is clearly line-of-sight elongation in both the Virgo and Fornax spiral population, (and insufficient information on Leo I). The distance dispersion works out at 0.38 mag in distance modulus. The ellipsoidal model of Gonzalez & Faber, sampled with the standard conical field-of-view, predicts such a dispersion with major axis scale length, b = 3 Mpc, when the minor axis scale length, a = 1 Mpc. Gonzalez & Faber assumed a = 1, and b = 2.5–4 Mpc. Our 11 galaxy sample has allowed us to narrow the range of b in the cluster model. For fields-of-view of diameter between 8° and 12°, the bias due to the geometrical extension of the cluster is 0.08 to 0.10 mag (4–5% in distance), in the sense that underestimated cluster distances will tend to bias H_0 high.

Gonzalez & Faber also noted another potential source of bias, the selection of the Virgo cluster itself. This selection results in a Malmquist bias of the conventional type present in homogeneous distributions of sampled objects (in this case galaxy clusters). Now that we have 3 clusters with distance uncertainties 0.04–0.14 mag, correction for this bias (by $1.38\sigma^2$ mag) can be neglected. As Gonzalez & Faber foresaw, "this particular bias correction is only of temporary interest, as Virgo will soon cease to be the lynch-pin of the Key Project."

In summary, we adopt a 5% downward correction, as determined from the modeling described above. Given the uncertainties in the line-of-sight structure of Virgo and Fornax, we assume the uncertainty in this correction is also $\pm 5\%$. This uncertainty may be conservative, given that our estimate for the bias is in agreement with values determined empirically by Tonry *et al.* (1999) and Ferrarese *et al.* (1999).

9. THE ERROR BUDGET AND THE FINAL VALUE OF THE HUBBLE CONSTANT

The goal of the Key Project is to measure a value for H_0 with a realistic uncertainty at or below 10%. In Table 3, we list an extensive error budget for this determination of the Hubble constant. The table has three sections, outlining the various stages of the measurement of H_0 using the fundamental plane and D_n-σ. In the first stage, we outline the typical error budget for a Cepheid distance measurement. The systematic errors in the Cepheid distance scale propagate directly to the value of H_0. These systematics include the uncertainty in the LMC distance, and the WFPC2 photometric zero points, which have been used in nearly all of the Key Project distance determinations. The total systematic error in the Cepheid distance scale amounts to $\pm$7% in H_0. The random errors in the Cepheid distances are treated as uncorrelated from galaxy to galaxy, and thus decrease by $\sqrt{N}$, when using N galaxies to measure the distance to a group or cluster. The individual random errors in the Cepheid distances used here were listed in Table 2, and are combined to provide the random errors in the distances to Leo I, Virgo, and Fornax given in Table 3.

The second section of the error budget lists components from each step in the derivation of the local fundamental plane and D_n-σ zero points. In the following sections, we attempt to quantify all the sources of error which propagate into uncertainties in our derived value of H_0. In particular, we estimate the impact on H_0 arising from systematic errors in the velocity dispersions and photometry of the calibrating galaxies, with respect to equivalent measurements made of the distant cluster samples. We also discuss the uncertainties due to the peculiar velocity field in the distant sample, and uncertainties due to errors in the fundamental plane slope.

Following the detailed discussion, we summarize the total uncertainties and provide the final, corrected value for the local expansion rate.

9.1. *Velocity Dispersions*

The largest single source of systematic error in the fundamental plane component of our analysis is in the comparison of the velocity dispersions of the calibrating galaxies with the distant ones. Fortunately, the exponent on σ in the fundamental plane is small, of order unity, and small systematic errors in σ remain as small systematic errors in H_0. This aspect can be contrasted to the Faber-Jackson and Tully-Fisher relations (Faber & Jackson 1976, Tully & Fisher 1977), for which the exponents are 3-4, causing errors in the internal kinematics to lead to large errors in derived distances.

Jørgensen *et al.* (1995a) attempted to homogenize the wealth of velocity dispersion information in the literature and made a detailed study of the systematic differences between existing kinematic datasets. They found that, in general, the Dressler *et al.* (1987) measurements obtained at LCO were quite good, with small systematic offsets between Dressler *et al.* and Jørgensen *et al.*. The mean offsets for the two sets of LCO dispersions were equivalent to +3% and −4% in distance, with *rms* scatter of $\pm$7% and $\pm$9%. Such scatter leads to uncertainties in the fundamental plane zero points of $\pm$2% and $\pm$3%. The velocity dispersions of the Virgo and Fornax galaxies used in this paper were derived primarily from LCO observations so we anticipate that these uncertainty estimates are appropriate for our analysis. The Fisher (1997) measurements in Leo I were performed with the same algorithm as the Jørgensen *et al.* (1995a) system and thus are expected to have negligible systematic uncertainties as well. We expect that any resulting systematic errors due to the differences in the systems of velocity dispersions are going to be at the level of 3-4%.

The aperture corrections we applied were generally small, but small uncertainties may remain and lead to errors in H_0. The Dressler *et al.* (1987) dispersions were measured in $16'' \times 16''$ apertures, equivalent to a circular aperture of $D = 18''.5$ (Jørgensen *et al.* 1995a). For the Virgo galaxies, this aperture is equivalent to $D = 3''.3$ at the distance of Coma; for the Fornax galaxies it is $D = 4''.3$. The *rms* scatter in the Jørgensen *et al.* (1995) modeling indicates that the uncertainties in the aperture corrections for Virgo and Fornax are less than 1%. (Jørgensen 1999, private communication). For the two Fisher (1997) galaxies, we applied aperture corrections of about 9%. The *rms* scatter in the Jørgensen *et al.* (1995) aperture corrections indicates that the uncertainty in the aperture corrected velocity dispersion for such large corrections is less than $\pm$6% per galaxy. Dividing by $\sqrt{2}$, we find a net effect of 4%. This uncertainty is diluted by the addition of the Faber *et al.* (1989) galaxies, whose velocity dispersions were obtained through apertures larger by a factor of three. Using these two galaxies, the net uncertainty due to the aperture corrections is less than 3%. The total uncertainty in the Leo I Fundamental Plane zero point due to aperture corrections is less than $\pm$0.02 dex. Averaged over the three groups/clusters, the net error due to the aperture corrections is likely to be on the order of, or less than $\pm$0.01 dex.

The level of rotational support in these galaxies can contribute to the scatter in the fundamental plane, but will not lead to systematic errors because the aperture corrections implicitly include both the gradient in velocity dispersion, and the variation of rotational support with radius. The gradient in the *total* second moment of the line-of-sight velocity distribution is a regular, smooth function, with little actual dependence on the level of rotational support and galaxy morphology, unlike the gradients in σ alone (Kelson *et al.* 1999c). Furthermore, the ranges of rotational support seen in each cluster are broadly consistent with each other (*e.g.*, Bender, Saglia, & Gerhard 1994, D'Onofrio *et al.* 1995, Fisher 1997). We conclude that errors in H_0 due to uncertainties in the aperture corrections are most likely small at a ~2%.

9.2. *Structural Parameters*

Differences in measurement techniques can lead to large random errors in the individual measurements of effective radii and surface brightnesses. The systematic offsets between these measurements made by different authors are typically small, at the level of few percent, despite potentially large uncertainties in the true half-light radius of a given galaxy (greater than 50% is not uncommon at times). Nevertheless, the combination of θ_e and $\langle I \rangle_e$ that appears in the fundamental plane is very stable given that the correlation coefficient between $\log\theta_e$ and $\log\langle I \rangle_e$ is −0.73. The systematic errors in this quantity, evidenced by differences between various authors, are typically at the level of a few percent, depending on the quality of the photometry/imaging data. The random errors are typically a few percent as well, tested by fitting different profile shapes to galaxies and re-deriving values of $r_e \langle I \rangle_e^{-0.82}$.

9.3. *Photometry*

There are several sources of uncertainty which can arise in the derivation of the Gunn r surface brightnesses themselves.

These include the initial calibration by Tonry *et al.* (1997), uncertainties in the transformation to Gunn *r*, errors in the galaxy colors, or in the assumption that color gradients in the galaxies are negligible. Each of these sources of error are discussed below in the context of our error budget.

9.3.1. *Calibration*

The Tonry *et al.* (1997) photometric system referenced to the system of Landolt (1992), the same system referred to by Jørgensen (1994), who explicitly derived transformations from the Landolt (1992) Johnson-Kron-Cousins system to the Thuan & Gunn (1976) photometric system. This suggests that systematic errors between the photometric systems of Tonry *et al.* (1997) and Jørgensen (1994) are very small. Tonry *et al.* (1997) quote uncertainties in the V photometric zero point of $\pm$2% and errors in $(V-I_c)$ of $\pm$2% and these are likely to propagate into systematic uncertainties in the Hubble constant.

9.3.2. *Transformation to Gunn r Photometry*

Jørgensen (1994) reported an *rms* scatter in their photometric transformation of approximately $\pm$0.02 mag. We can test the validity of the transformation by reversing the direction of the transformation, and re-measuring the Hubble constant. Earlier, the V and I_c colors were used to transform the Leo I, Virgo, and Fornax data to Gunn *r*, for direct comparison to the Jørgensen *et al.* database. However, a subset of 28 galaxies in Coma also have $B-r$ colors. Thus, we can transform these to Johnson V, for direct comparison with the Leo I, Virgo, and Fornax galaxies. In this way, we explicitly test the systematic uncertainties of Eq. 5, as well as our approximation of $(B-V) \approx 0.814(V-I_c)$. The net effect on the Hubble constant is less than 2%. Thus, we adopt an error estimate of 2% for our error budget. We note that this test is not independent of the accuracy of the $B-r$ colors of the Jørgensen *et al.* Coma galaxies.

9.3.3. *Consistency of Galaxy Colors*

A subset of 28 Coma galaxies have both Gunn *r* and Johnson *B* photometry. Using these data, we find that the mean $V-r$ colors of Coma early-type galaxies is $\langle V-r \rangle = 0.198 \pm 0.002$ mag (internal error only). We can compute the mean $V-r$ colors of the Leo I, Virgo, and Fornax galaxies using Eq. 5 and rewriting it as

$$(V-r) = -0.273 + 0.396 \times (V-I_c) \qquad (7)$$

We report mean $(V-r)$ colors for the galaxies in Leo I, Virgo, and Fornax of 0.177 ± 0.013 mag, 0.185 ± 0.005 mag, 0.195 ± 0.005 mag (again, these are the internal errors). The uncertainties on the colors themselves are on the order of $\pm$0.01 to $\pm$0.02 mag. This similarity in the galaxy colors suggest a remarkable uniformity in the stellar populations (*e.g.*, Bower, Lucey, & Ellis 1992). Given the consistent galaxy colors, we conclude that the Gunn *r* surface brightnesses are likely to be good to $\pm$0.02 mag.

9.3.4. *The Effect of Color Gradients*

One issue that has not been addressed is the assumption that color gradients are negligible. In §3.2.3, we noted that the color gradients were indeed small. We can explicitly test their effects by measuring the structural parameters in the I_c band, transforming the I_c-band surface brightnesses to Gunn *r* using the $(V-I_c)$ colors, and re-deriving the fundamental plane zero points. For the Virgo galaxies, there is less than a 1% change in the zero point of the fundamental plane. For the Fornax galaxies, there is a net change of 2.5%. This test is not independent of the any errors in the photometric transformation, but given the previous discussions, none of these uncertainties lead to large errors in H_0.

9.4. *Systematic Uncertainties due to the Velocity Field*

Using the fundamental plane, we derived identical values for the Hubble constant using recession velocities for the distant clusters in both the CMB reference frame, and in the frame of the flow-field model of Mould *et al.* (1999). In order to establish our estimate of the error due to uncertainties in the velocity field, we studied those distant clusters with more than 20 galaxies and found a standard deviation of 4% in their implied values of the Hubble constant. This scatter is a combination of the random uncertainties in the distant zero points due to the finite numbers of galaxies, and the errors due to the random motions of the clusters on top of the smooth Hubble flow. We conservatively adopt the 4% as the random error in a measurement of the Hubble constant from a single distant cluster. We assume that this uncertainty decreases with the square-root of the number of distant clusters and adopt an error in final determination of H_0 of 1%.

9.5. *Uncertainties in the Slope of the Fundamental Plane and D_n-σ Relations*

The fundamental plane is essentially a relation between M/L ratio and galaxy mass (Faber *et al.* 1987). In order for the fundamental plane to be effective as a distance indicator, this scaling between M/L and the structural parameters must be consistent from cluster to cluster. If M/L scales differently in any of the clusters, then for a given value of σ and θ_e, the predicted M/L will not be correct, and the deduced distance will be incorrect as well. We now consider uncertainties in the fundamental plane slope, and their impact on our value of the Hubble constant.

Varying the slope on $\log\sigma$ from 1.14-1.30 (the $\pm$1-σ range in Jørgensen *et al.* 1996) amounts to a 1% variation in the Hubble constant. The published uncertainty in β of $\pm$0.02 also leads to negligible changes in the Hubble constant.

However, there remains an ambiguity in that we have two scaling relations, the FP and D_n-σ, which are not equivalent in shape but have similar scatter (*e.g.*, $\pm$10% in distance in Virgo). We also noted that there is a specific relationship $\theta_n = f(\theta_e, \langle I \rangle_e)$ with a slope which is different from the value of β in the fundamental plane. Thus, we now experiment with revised forms of the fundamental plane by fixing $\beta = -0.73$, the value implicit in D_n-σ.

Taking the Coma data of Jørgensen *et al.* (1995ab) and performing a linear least squares fit, to those galaxies with $\log\sigma > 2$, we find the following D_n-σ relation

$$\log\theta_n \propto (1.22 \pm 0.08)\log\sigma \qquad (8)$$

This relation corresponds to a fundamental plane of the form $\log\theta_e = 1.22\log\sigma - 0.73\log\langle I \rangle_e$.

Using this new plane, we find (metric) zero points for Leo I, Virgo, and Fornax of $\langle\gamma\rangle_{\rm LeoI} = -0.309 \pm 0.042$, $\langle\gamma\rangle_{\rm Virgo} = -0.371 \pm 0.013$, $\langle\gamma\rangle_{\rm Fornax} = -0.345 \pm 0.033$. The new (angular) zero point for Coma is $\langle\gamma\rangle_{\rm Coma} = -5.325 \pm 0.010$. The net effect on the Hubble constant is –2.5%.

The small impact on the Hubble constant that arises when the fundamental plane coefficients are adjusted is largely due to the

averaging of the zero points in the three clusters. By setting the zero point to only one of the clusters alone, values of H_0 may vary over a slightly broader range. The Fornax cluster, with its large scatter, is the worst case. Given the large scatter in Fornax, a modest change in β will lead to larger zero point shifts because of the correlation between θ_e and $\langle I \rangle_e$. The shift from $\beta = -0.82$ to $\beta = -0.73$ decreases its Hubble constant by 6%. Given the scatter in the Fornax FP, this offset is not statistically significant.

Averaging over the Leo I, Virgo, and Fornax diminishes the uncertainty in H_0 due to errors in the FP slopes primarily because the scatter in the Virgo relation is so low. Nevertheless, we conclude that uncertainties in the fundamental plane slopes are at most a small contributor to the total error in the Hubble constant itself.

9.6. *The Total Error in H_0*

Given the level of uncertainties listed in Table 3, an accuracy of $\pm$10% cannot be achieved using the fundamental plane or D_n-σ relations alone. The largest single sources of error are currently systematic: (1) the LMC distance, (2) the WFPC2 photometric calibration, (3) the Cepheid metallicity correction, and (4) depth effects between the spirals and ellipticals. The systematic errors in the Cepheid distance scale, including the uncertainty in the LMC distance, combine to a total of $\pm$7%. The random errors in the Cepheid distances do not contribute much to the total random error in H_0; it is the superposition of the random small errors in the FP (and D_n-σ) which make up the bulk of the total random uncertainty of $\pm$6%. Remaining systematic uncertainties arising from the fundamental plane analysis and the systematic corrections, when combined in quadrature, amount to about $\pm$8%, leading to a total systematic uncertainty in H_0 of $\pm$11%.

However, by combining several independent distance indicators, the goal of the Key Project may be realized (Mould *et al.* 1999). Each method provides its own set of constraints and systematic uncertainties on the value, thereby reducing the total uncertainty in the Hubble constant. This subject is the focus of Mould *et al.* (1999a) and Freedman *et al.* (1999), who attempt to combine all of the constraints provided by this work, Ferrarese *et al.* (1999), Gibson *et al.* (1999), and Sakai *et al.* (1999).

9.7. *A Final Value for the Hubble Constant*

In §5, we used the fundamental plane in Leo I, Virgo, and Fornax to set the distance scale. Upon comparing the zero points of the distant clusters to the one defined by the calibrating galaxies, we determined a raw value of $H_0 = 82 \pm 5 \pm 10$ km s^{-1}Mpc^{-1}. However, we also estimated to what extent the value of H_0 is likely to be biased by the assumption that the Key Project spirals may be used to set distances to the three clusters used in this paper, and concluded that the raw value for the expansion rate is likely to be biased by approximately $-5\% \pm 5\%$. We therefore correct the estimate of H_0 derived in §5 and arrive at our adopted value of $H_0 = 78 \pm 5 \pm 9$ km s^{-1}Mpc^{-1}. Adoption of the Kennicutt *et al.* (1998) metallicity correction, would further reduce this value to $H_0 = 73 \pm 4 \pm 9$ km s^{-1}Mpc^{-1}.

10. COMPARISONS WITH THE LITERATURE

Our value of H_0 using Leo I alone can be compared directly with that of Hjorth & Tanvir (1997), who used a Cepheid distance to NGC 3368 of 11.6 ± 0.9 Mpc. Our distance is 5% shorter. Had Hjorth & Tanvir (1997) adopted the Key Project distance to Leo I, and the flow-field velocity of cz_{flow} = 7392 km s^{-1}, they would have found $H_0 = 77 \pm 9$ km s^{-1}Mpc^{-1} instead of $H_0 = 67 \pm 8$ km s^{-1}Mpc^{-1}. Using Leo I alone and Coma, we find $H_0 = 70 \pm 4$ km s^{-1}Mpc^{-1} (internal). This 10% discrepancy can arise from either the photometry or the velocity dispersions. Comparing values of $\theta_e \langle I \rangle^{0.82}$ in Gunn *r*, our values differ from those of Hjorth & Tanvir (1997) by only 1% in the mean. This comparison is remarkable considering our error estimate of 5% in Table 3.

The discrepancy between the Hjorth & Tanvir (1997) result and ours can be attributed solely to a systematic difference in the aperture-corrected velocity dispersions. For NGC 3377 and NGC 3379, the comparison is quite good; our aperture-corrected velocity dispersions agree to 3%. For NGC 3384 and NGC 3412, the comparison is quite poor; our aperture-corrected values are 20% lower than Hjorth & Tanvir's estimates. According to our error budget, we estimated that the total systematic uncertainty in the velocity dispersions was of order 5%. Perhaps the correction for apertures as small as those used by Fisher (1997) is uncertain by more than we estimated. Jørgensen *et al.* (1995) approximated the correction from small-aperture velocity dispersions to equivalent large-aperture measurements using a sample of 51 nearby galaxies. The power-law they derived is the median relation for that sample, and we used the *rms* scatter about this relation to estimate our uncertainties in §9. Perhaps the uncertainties in the Hjorth & Tanvir (1997) estimated corrections are larger than those authors assumed.

We can also compare our results to that of Gregg (1995). Using the *K*-band D_n-σ relation, he inferred a relative Coma-Virgo distance of 5.56 (no error estimate). Using the fundamental plane, we find 5.57 ± 0.50, and using D_n-σ, we find 5.87 ± 0.52, both of which are in excellent agreement.

Another test of our analysis can be made by comparing our structural parameters with those of Faber *et al.* (1989), who reported values of A_e (effective diameter $\equiv 2 \times \theta_e$) and Σ_e (the *B*-band surface brightness within A_e) for a large sample of early-type galaxies, include several in Leo I, Virgo, and Fornax. Using $(B-V) \approx 0.814 \times (V-I_c)$ and the Jørgensen (1994) transformation, we can correct the *B*-band surface brightnesses to Gunn *r*, and compare fundamental planes.

Faber *et al.* only report data for two galaxies in Leo I, N3377 and N3379. Using these two galaxies, there is a systematic difference between our photometry and theirs of –4% in distance. However, given only two galaxies, it is difficult to evaluate the significance of this discrepancy. For the Virgo galaxies, the comparison is quite favorable. The Faber *et al.* (1989) data, transformed to Gunn *r*, produce a fundamental plane zero point only offset –3% in distance from the one derived earlier from the Tonry *et al.* (1997) photometry. This offset is statistically insignificant. For the Fornax galaxies, the offset is $-11\% \pm 4\%$ (internal error only). In §9, we estimated that our fundamental plane parameters may have uncertainties on the order of $\pm$5%. We have no estimates for the uncertainties in the Faber *et al.* (1989) photometry, so the errors on the Fornax offset given above is a lower limit. We also note that the scatter in the Virgo and Fornax fundamental planes, derived from the Faber *et al.* data is identical to what was derived earlier using the Tonry *et al.* (1997) photometry.

D'Onofrio *et al.* (1997) used the *B* band D_n-σ and fundamental plane relations to determine the Virgo-Fornax relative distance modulus. Using the fundamental plane, they found

a relative modulus of $\mu_{FV} = 0.45 \pm 0.15$ mag. The fundamental plane zero points we find for Virgo and Fornax imply $\mu_{FV} = 0.52 \pm 0.17$ mag. Given this agreement, we conclude that the disagreement between our data and Faber *et al.* (1989) for the Fornax galaxies may point to larger uncertainties in the Faber *et al.* (1989) dataset than anticipated. We also note that D'Onofrio *et al.* (1997) find values for the scatter in the Virgo and Fornax fundamental plane relations that are similar to ours.

11. CONCLUSIONS

Using the fundamental plane relations in Leo I, Virgo, and Fornax and comparing the 11 clusters of Jørgensen *et al.* (1995), we found a raw value for the local Hubble constant of $82 \pm 5 \pm 10$ km s^{-1}Mpc^{-1} (random, systematic). Correcting for depth effects in the nearby clusters, we estimate that the local expansion rate is $5\% \pm 5\%$ smaller and conclude that $H_0 = 78 \pm 5 \pm 9$ km s^{-1}Mpc^{-1}.

The largest systematic uncertainties come from the LMC distance, the WFPC2 calibration, the metallicity correction to the two-color Cepheid distances, and the uncertainty in the Cepheid distances to the three nearby clusters. By adopting the Kennicutt *et al.* (1998) metallicity correction the distances to Leo I, Virgo, and Fornax decrease by $8\% \pm 5\%$, $6\% \pm 4\%$, and $4\% \pm 3\%$, respectively. The net effect would be to decrease the Hubble constant by $6\% \pm 4\%$ to $H_0 = 73 \pm 4 \pm 9$ km s^{-1}Mpc^{-1}.

The distant cluster sample spans a wide range of recession velocities, from $cz \approx 1100$ km s^{-1}to $cz \approx 11000$ km s^{-1}, with a mean $cz \approx 6000$ km s^{-1}. The value of H_0 using either the CMB, or the flow-field model of Mould *et al.* (1999a) as the preferred reference frame, give the same value to within 1%. Using Coma with its CMB velocity, yields a value for the local expansion rate which is nearly 4% smaller. However, using the flow-field reference frame, Coma yields the same value of the Hubble constant as the weighted mean of the 11 clusters, to within less than 1%. Therefore, by using all 11 clusters of Jørgensen *et al.* (1996), we anticipate that uncertainties due to the peculiar velocity field are likely to be at a level of 1%.

When using the D_n-σ relation, we find a value which is smaller by 4%, but the D_n-σ relation is a curved projection of the fundamental plane (Jørgensen *et al.* 1993, and this paper). Thus, the fundamental plane is preferred and appears to be a more accurate secondary distance indicator, particularly when care is taken to minimize, and quantify the systematic errors.

The values of H_0 given above were derived by fixing the fundamental plane and D_n-σ relations' zero points to the Cepheid distances to Leo I, Virgo, and Fornax spirals. The Cepheid distance to Fornax is defined by NGC 1365, NGC 1326A and NGC 1425. The distance modulus to NGC 1425 is 0.4 mag larger than the former two. Suntzeff *et al.* (1999) have suggested that the hosts of Ia supernovae may lie several tenths of a magnitude beyond NGC 1365. Thus, if the ellipticals used in this paper are at the distance of NGC 1425, then the Hubble constant, derived using a weighted mean of the three calibrating clusters, decreases by 2%. If the Fornax ellipticals are at the distance of the nearer of the two Cepheid distances then the Hubble constant increases by about 2%.

While our uncertainty on the Hubble constant ($H_0 = 78 \pm 5 \pm 9$km s^{-1}Mpc^{-1}) from this single distance indicator is greater than 10%, these results will be combined by Mould *et al.* (1999a) and Freedman *et al.* (1999) with results from the Type Ia Supernovae (Gibson *et al.* 1999), Tully-Fisher relation (Sakai *et al.* 1999), and surface-brightness fluctuation method (Ferrarese *et al.* 1999) to produce a more accurate value of the local expansion rate of the Universe.

We gratefully the advice of A. Gonzalez in estimating the uncertainty in the spatial coincidence of spirals and ellipticals. The work presented in this paper is based on observations with the NASA/ESA Hubble Space Telescope, obtained by the Space Telescope Science Institute, which is operated by AURA, Inc. under NASA contract No. 5-26555. We gratefully acknowledge the support of the NASA and STScI support staff, with special thanks to our program coordinator, Doug Van Orsow. Support for this work was provided by NASA through grant GO-2227-87A from STScI. SMGH and PBS are grateful to NATO for travel support via Collaborative Research Grant 960178. LF acknowledges support by NASA through Hubble Fellowship grant HF-01081.01-96A awarded by the Space Telescope Science Institute, which is operated by the Association of Universities for Research in Astronomy, Inc., for NASA under contract NAS 5-26555. This research has made use of the NASA/IPAC Extragalactic Database (NED) which is operated by the Jet Propulsion Laboratory, California Institute of Technology, under contract with the National Aeronautics and Space Administration.

REFERENCES

Aaronson, M., Mould, J., & Huchra, J. 1979, ApJ, 229, 1
Bender, R., Saglia, R.P., & Gerhard, O.E. 1994, MNRAS, 269, 785
Bower, R.G., Lucey, J.R., & Ellis, R.S. 1992, MNRAS, 254, 601
Burstein, D., Faber, S.M., & Dressler, A. 1990, ApJ, 354, 18
Caon, N., Capaccioli, M., & D'Onofrio, M. 1993, MNRAS, 265, 1013
Cardelli, J. A., Clayton, G. C., & Mathis, J. S. 1989, ApJ, 345, 245
Ciotti, L. & Lanzoni, B., 1997, A&A, 321, 724
Colless, M., & Dunn, A.M. 1996, ApJ, 458, 435
Davies, R., 1981, MNRAS, 194, 879
Davies, R., Burstein, D., Dressler, A., Faber, S.M., Lynden-Bell, D., Terlevich, R.H. & Wegner, G. 1987, ApJS, 64, 581
de Vaucouleurs, G. 1961, ApJS, 5, 233
de Vaucouleurs, G. & Olson, D. 1982, ApJ, 256, 346
Djorgovski S., & Davis M. 1987, ApJ, 313, 59
Djorgovski, S., de Carvalho, R. & Han, M.-S. 1988, in "The Extragalactic Distance Scale" ed. S. van den Bergh & C.J. Pritchet (ASP Conf. Ser., 4), 329
D'Onofrio, M., Zaggia, S.R., Longo, G., Caon, N., Capaccioli, M. 1995, A&A, 296, 319
D'Onofrio, M., Capaccioli, M., Zaggia, S.R., & Caon, N. 1997, MNRAS, 289, 847
Dressler, A. 1984, ApJ, 281, 512
Dressler, A., Lynden-Bell, D., Burstein, D., Davies, R.L., Faber, S.M, Terlevich, R.J. & Wegner, G. 1987, ApJ, 313, 42
Faber, S.M. & Jackson, R.E. 1976, ApJ, 204, 668
Faber S. M., Dressler A., Davies R. L., Burstein D., Lynden-Bell D., Terlevich R., & Wegner G. 1987, Faber S. M., ed., Nearly Normal Galaxies. Springer, New York, p. 175
Faber, S.M., Wegner, G., Burstein, D., Davies, R.L., Dressler, A., Lynden-Bell, D., & Terlevich, R.H. 1989, ApJS, 69, 763
Federspiel, M., Sandage, A. & Tammann, G.A. 1994, ApJ, 430, 29
Ferrarese, L., *et al.* 1996, ApJ, 464, 568
Ferrarese, L., *et al.* 1999, ApJ, accepted for publication
Fisher, D. 1997, AJ, 113, 950
Freedman, W. L., *et al.* 1999, ApJ, in preparation
Frei, Z., & Gunn, J.E. 1994, AJ, 108, 1476
Fukugita, M.,Hogan, C.J., & Peebles, P.J.E. 1993, Nature, 366, 309
Gibbons, R.A, Fruchter, A.S., & Bothun, G.D. 1998, astro-ph/9903380
Gibson, G. 1999, ApJ, accepted for publication
Graham, A., & Colless, M. 1997, MNRAS, 287, 221
Gonzalez, A.H., & Faber, S.M. 1997, ApJ, 485, 80
Graham, J., *et al.* 1997, ApJ, 477, 535
Graham, J., *et al.* 1999, ApJ, in press
Gregg, M.D. 1992, ApJ, 384, 43
Hanes, D.A., & Whittaker, D.G. 1987, AJ, 94, 906

Hjorth, J. & Tanvir, N.R. 1997, ApJ, 482, 68
Holtzman, J.A., *et al.* 1995, PASP, 107, 1065
Hudson, M.J., Lucey, J.R., Smith, R.J., & Steel J. 1997, MNRAS, 291, 488
Jacoby, G.H. 1989, ApJ, 339, 39
Jacoby, G.H., *et al.* 1992, PASP, 104, 599
Jørgensen I., Franx M., & Kjærgaard P. 1992, A&AS, 95, 489
Jørgensen I. 1994, PASP, 106, 967
Jørgensen I., Franx M., & Kjærgaard P. 1993, ApJ, 411, 34
Jørgensen I., Franx M., & Kjærgaard P. 1995a, MNRAS, 273, 1097
Jørgensen I., Franx M., & Kjærgaard P. 1995b, MNRAS, 276, 1341
Jørgensen I., Franx M., & Kjærgaard P. 1996, MNRAS, 280, 167 [JFK96]
Jørgensen I. 1999, private communication
Kelson, D.D., 1998, Ph.D. thesis, Univ. of California, Santa Cruz
Kelson, D.D., 1999, ApJ, in preparation
Kelson, D.D., *et al.* 1999a, ApJ, in press
Kelson, D.D., *et al.* 1999b, ApJ, submitted
Kelson, D.D., *et al.* 1999c, ApJ, submitted
Kennicutt, R.C., *et al.* 1998, ApJ, 498, 181
Landolt, A., 1992, AJ, 104, 372
Lucey, J.R., Bower, R.G., & Ellis, R.S. 1991, MNRAS, 249, 755
Lynden-Bell, D., Faber, S.M, Burstein, D., Davies, R.L., Dressler, A., Terlevich, R.J. & Wegner, G. 1987, ApJ, 326, 19
Macri, L.M., *et al.* 1999, ApJ, in press
Maia, M.A.G., da Costa, L.N., Latham, D.W. 1989, ApJS, 69, 809
Madore, B.F. & Freedman, W.L. 1999, ApJ in preparation
Mould, J.R. 1999a, ApJ, submitted
Mould, J.R. 1999b, ApJ, submitted
Pahre, M.A., 1998, Ph.D. thesis, California Inst. of Technology
Prosser, C., *et al.* 1999, ApJ, submitted
Renzini, A., & Ciotti, L. 1993, ApJ, 416, 49
Riess, A.G., Press, W.H., & Kirshner, R.P. 1996, ApJ, 473, 88
Saglia, R.P., *et al.* 1997, ApJS, 109, 79
Sandage, A.R., & Visvanathan, N. 1978, ApJ, 225, 742
Sakai, S. 1999, ApJ, accepted for publication
Schlegel, D.J., Finkbeiner, D.P., & Davis, M. 1998, ApJ, 500, 525
Sersic, J.L. 1968, *Atlas de Galaxia Australes*, (Cordoba: Observatorio Astronomico)
Silbermann, N., *et al.* 1999, ApJ, 515, 1
Suntzeff, N. B., *et al.* 1999, AJ, in press
Terlevich, R.J., Davies, R.L., Faber, S.M., & Burstein, D. 1981, MNRAS, 196, 381
Thuan T.X., & Gunn, J., 1976, PASP, 88, 543
Tonry, J., & Davis, M. 1981, ApJ, 246, 680
Tonry, J. 1983, ApJ, 266, 58
Tonry, J., & Schneider, D.P. 1988, AJ, 96, 807
Tonry, J., Blakeslee, J.P., Ajhar, E.A., & Dressler, A. 1997, ApJ, 475, 399
Tonry, J., Blakeslee, J.P., Dressler, A., & Ajhar, E.A., 1999, in preparation
Trager, S.C. 1997, Ph.D. thesis, Univ. Calif., Santa Cruz
Tully, R.B. & Fisher J.R. 1977, A&A, 54, 661
van Dokkum, P.G., Franx, M., Kelson, D.D., & Illingworth, G.D. 1998, ApJ, 504, 17
Wegner, G., Colless, M., Baggley, G., Davies, R.L, Bertschinger, E., Burstein, D., McMahan, R.K., Jr., & Saglia, R.P. 1996, ApJS, 106, 1
Worthey, G., Trager, S. C., & Faber, S. M. 1996, in "Fresh Views on Elliptical Galaxies," eds. A. Buzzoni, A. Renzini, & A. Serrano, (ASP Conf. Ser., 86) p. 203

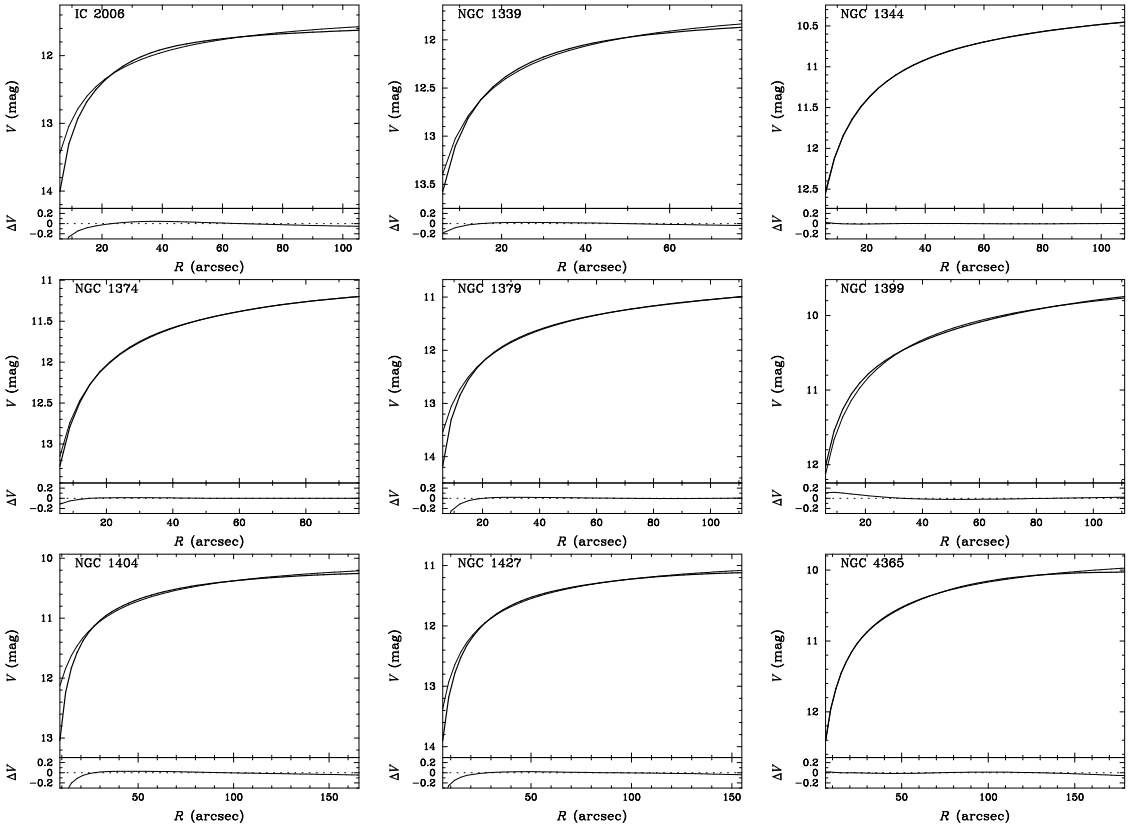

FIG. 1.— The Johnson *V* circular aperture growth curves of Tonry *et al.* (1997) are shown as thick solid lines, while the integrated $r^{1/4}$-law profiles are shown as thin solid lines. In the lower panels, the residuals from the $r^{1/4}$-law fit are shown.

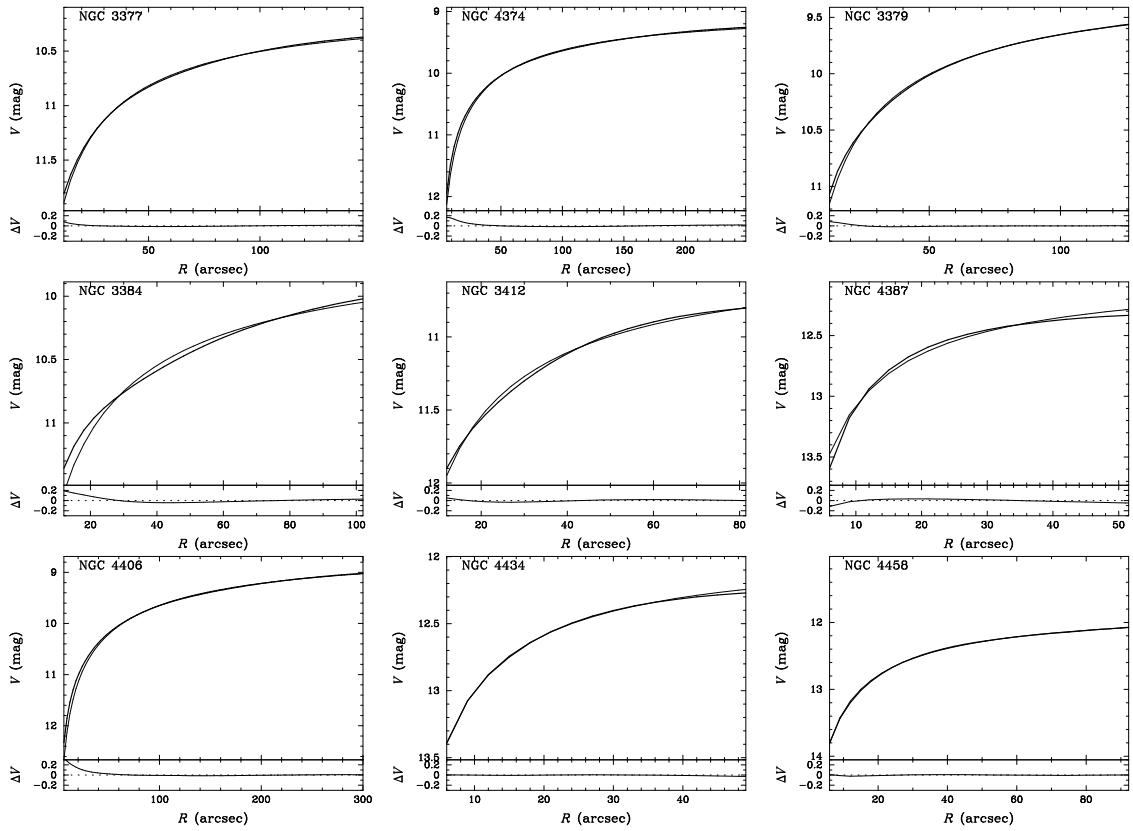

FIG. 1. (continued) —

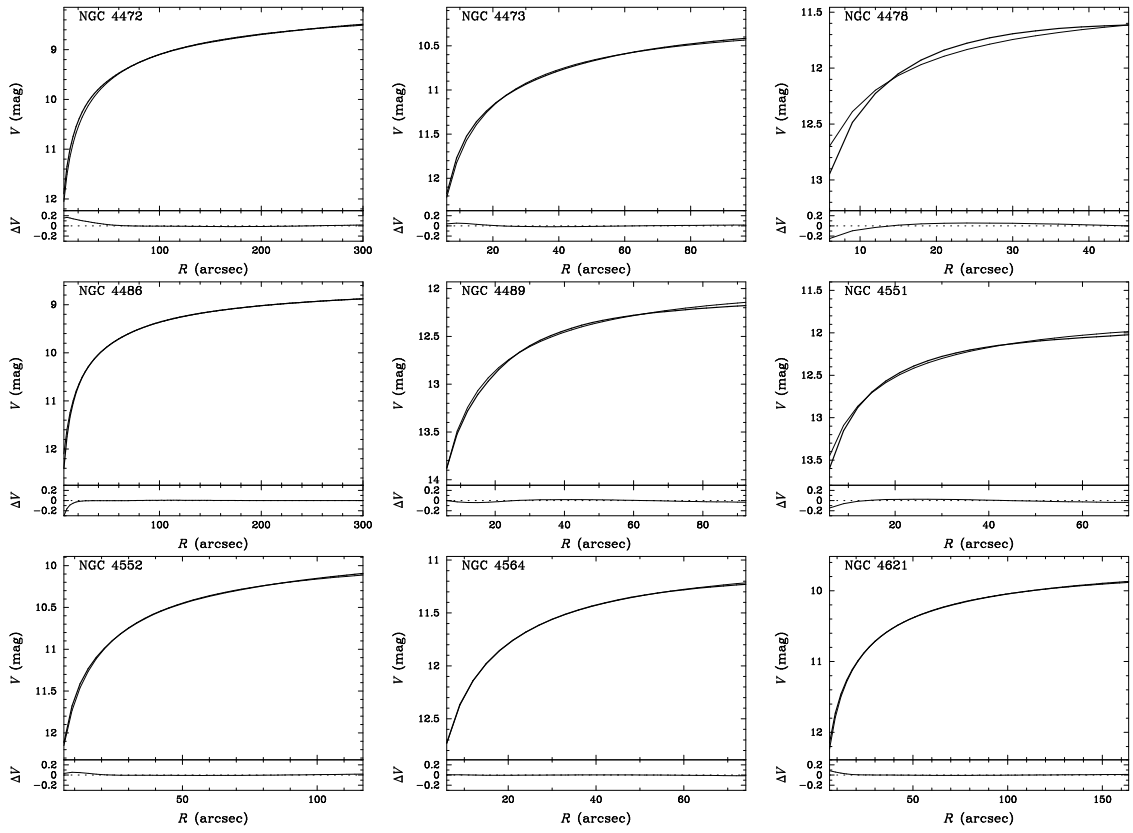

FIG. 1. (continued) —

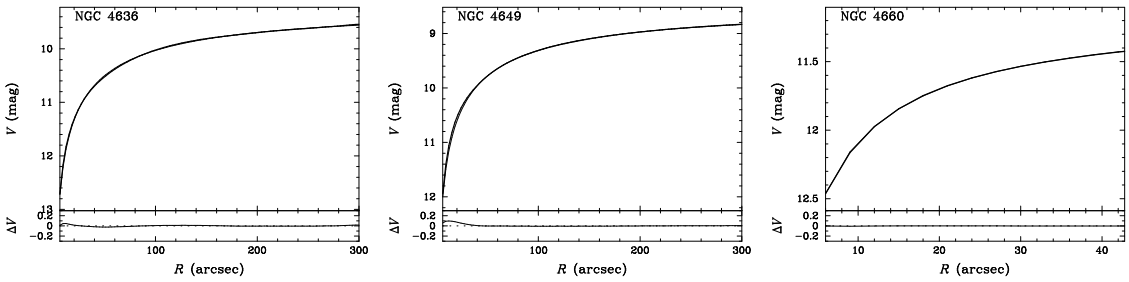

FIG. 1. (continued) —

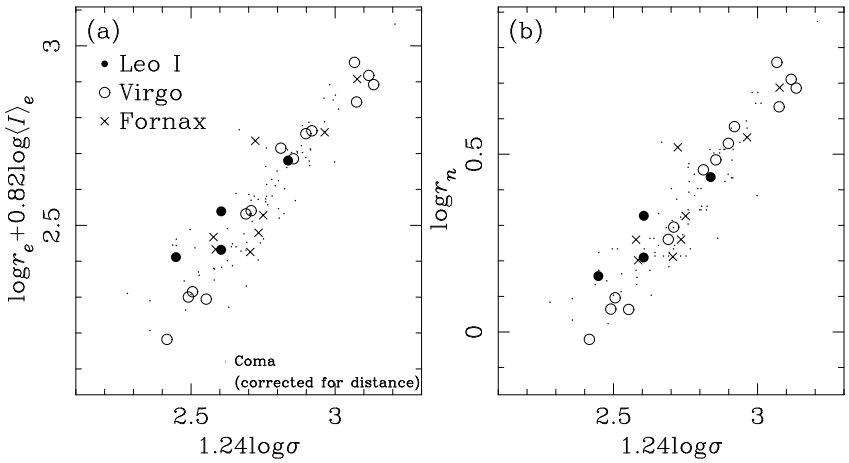

FIG. 2.— The (a) fundamental plane and (b) D_n-σ relations in Leo I, Virgo, and Fornax, where distance effects have been removed. The Coma sample from Jørgensen *et al.* (1995ab) is shown, corrected for distance, by small points.

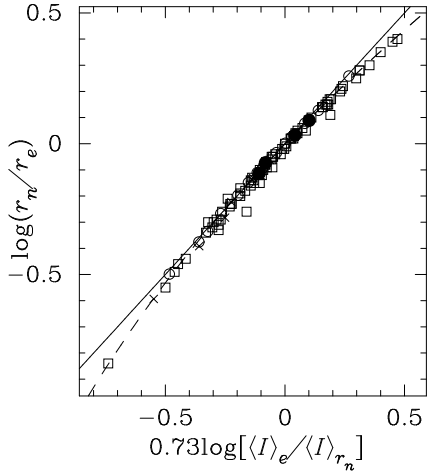

FIG. 3.— The relationship between r_n and r_e, $\langle I \rangle_e$. The symbols are as in Figure 2 with the addition of the Coma sample as squares. The solid line has a slope of unity, representing the leasts-squares fit to the data (see §6.3). The dashed line follows a pure $r^{1/4}$-law growth curve. Thus, the D_n-σ relation is a combination of the fundamental plane and the error correlation between r_e and $\langle I \rangle_e$.

TABLE 1
FUNDAMENTAL PLANE AND D_n-σ QUANTITIES

Galaxy	Type	V-band θ_e[a] (arcsec)	V-band $\langle\mu\rangle_e$[a] (mag/arcsec^2)	r-band θ_n (arcsec)	$\log\langle I\rangle_e$[b] $L_\odot/pc^2$[e]	$\log\sigma$[c] (km/s)	$(V-I_c)$ (mag)	$E(B-V)$ (mag)	cz[d] (km/s)
NGC 3377	E5	41.78 ± 0.53	20.28 ± 0.02	32.19	2.572	2.100	1.22	0.03	692
NGC 3379	E1	50.40 ± 0.64	19.76 ± 0.03	54.21	2.776	2.287	1.21	0.02	920
NGC 3384	SB0	49.91 ± 1.16	20.18 ± 0.05	42.20	2.609	2.101	1.17	0.03	735
NGC 3412	SB0	23.27 ± 0.61	19.54 ± 0.05	28.55	2.857	1.974	1.18	0.03	865
NGC 4365[f]	E3	51.10 ± 0.84	20.31 ± 0.03	38.86	2.552	2.409	1.22	0.02	1240
NGC 4374	E1	71.15 ± 0.53	20.33 ± 0.02	55.19	2.561	2.477	1.21	0.04	1000
NGC 4387	E5	14.72 ± 3.65	19.88 ± 0.49	14.85	2.726	2.056	1.17	0.03	561
NGC 4406	S0/E3	150.82 ± 0.80	21.52 ± 0.01	48.54	2.065	2.352	1.18	0.03	-227
NGC 4434	E0/S0	14.02 ± 3.76	19.76 ± 0.53	14.89	2.759	2.006	1.15	0.02	1071
NGC 4458	E0	26.36 ± 4.22	20.96 ± 0.32	12.24	2.280	1.946	1.15	0.02	668
NGC 4472	E2/S0	135.85 ± 0.43	20.81 ± 0.01	73.63	2.353	2.471	1.25	0.02	868
NGC 4473	E5	27.64 ± 0.96	19.43 ± 0.07	36.69	2.905	2.265	1.18	0.03	2240
NGC 4478	E2	12.92 ± 1.27	18.96 ± 0.18	23.38	3.085	2.167	1.17	0.03	1381
NGC 4486	Epec	98.27 ± 0.41	20.58 ± 0.01	62.29	2.449	2.525	1.25	0.02	1282
NGC 4489[g]	E	26.40 ± 4.50	21.03 ± 0.34	11.34	2.245	1.775	1.08	0.03	971
NGC 4551	E	19.96 ± 3.48	20.24 ± 0.34	16.02	2.589	2.018	1.18	0.04	1470
NGC 4552[h]	E	35.97 ± 0.81	19.66 ± 0.04	42.60	2.828	2.388	1.21	0.04	321
NGC 4564	E6	21.17 ± 1.70	19.63 ± 0.16	25.31	2.833	2.182	1.20	0.04	1111
NGC 4621	E5	46.82 ± 0.76	20.02 ± 0.03	43.57	2.675	2.335	1.20	0.03	424
NGC 4636	E/S0	92.94 ± 0.76	21.15 ± 0.02	39.13	2.227	2.300	1.27	0.03	1095
NGC 4649	E2	93.15 ± 0.40	20.44 ± 0.01	65.93	2.508	2.511	1.26	0.03	1413
NGC 4660[f]	E	12.25 ± 1.55	18.64 ± 0.25	26.02	3.225	2.259	1.20	0.03	1097
NGC 1339	E4	22.05 ± 3.04	20.31 ± 0.27	16.06	2.533	2.180	1.15	0.01	1367
NGC 1344	E5	40.06 ± 1.21	20.17 ± 0.06	32.66	2.594	2.194	1.15	0.02	1169
NGC 1374	E0	34.96 ± 2.19	20.62 ± 0.12	20.93	2.414	2.216	1.16	0.01	1352
NGC 1379	E0	70.38 ± 3.97	21.72 ± 0.12	17.95	1.969	2.077	1.16	0.01	1380
NGC 1399	E0	55.42 ± 0.94	20.10 ± 0.04	48.07	2.632	2.479	1.25	0.01	1447
NGC 1404	E2	47.34 ± 1.08	20.34 ± 0.05	34.83	2.535	2.388	1.24	0.01	1942
NGC 1427	E5	44.28 ± 2.25	21.07 ± 0.10	17.97	2.229	2.203	1.17	0.01	1416
IC 2006	E	30.10 ± 2.84	20.71 ± 0.19	15.71	2.377	2.083	1.20	0.01	1364

NOTE.— Hubble types taken from the RC3 and Ferguson (1989). The V-band photometry listed here has not been corrected for galactic extinction, nor for cosmological surface brightness dimming, nor have K-corrections been applied. The FP and D_n-σ zero points in Table 4 (γ, δ) were computed after taking these other effects into account.

[a] Errors in θ_e and $\langle\mu\rangle_e$ are strongly correlated, such that their combination in the fundamental plane remains conserved to a high degree of precision, even when errors in effective radius and surface brightness are large.

[b] Values of surface brightness are in units of solar luminosities per square parsec in the Gunn r band in the restframe of the galaxy.

[c] Values for $\log\sigma$ have been corrected to a nominal aperture of $D = 3''.4$ at the distance of Coma. Values of $\log\sigma$ for NGC 3377 and NGC 3379 were taken from Faber *et al.* (1989), and corrected using the more recent aperture corrections of Jørgensen *et al.* (1995a). The Virgo and Fornax $\log\sigma$ values are from Dressler *et al.* (1987) who derived dispersions from $16'' \times 16''$ apertures. The values for NGC 3412 and NGC 3384 were taken from Fisher *et al.* (1996), and corrected for aperture size from their aperture of $2'' \times 4''$ to the nominal aperture.

[d] Recession velocities, taken from NED, are used to compute the K-corrections and cosmological surface brightness dimming.

[e] $\langle I\rangle_e$, in solar luminosities per square parsec in the Gunn r band. Galactic exctinction has been removed. K-corrections were performed using the individual redshifts. Surface brightness dimming of $(1+z)^4$ has been removed using mean recession velocities for Leo I, Virgo, and Fornax, of 750 km s^{-1}, 1050 km s^{-1}, and 1400 km s^{-1}, respectively.

[f] SBF measurements of NGC 4365 and NGC 4660 indicate that they are not associated with the other members of Virgo (Tonry *et al.* 1997). These are disregarded in the FP and D_n-σ analysis.

[g] Too blue; dropped from subsequent analysis.

[h] The image of the core of NGC 4552 was saturated so the observed mean surface brightness and θ_n are in error; also dropped from subsequent analysis.

TABLE 2
CEPHEID DISTANCE MODULI TO LEO I, VIRGO, AND FORNAX GALAXIES

Galaxy	$(m-M)_0$[a] (mag)	$(m-M)_0$[b] (mag)	Random Error (mag)	Original Reference[c]
		Leo I		
NGC 3351	30.01	30.19	± 0.08	Graham *et al.* (1997)
NGC 3368	30.20	30.37	± 0.10	Gibson *et al.* (1999)
weighted mean	30.08	30.27	± 0.11	
		Virgo		
NGC 4321	31.04	31.19	± 0.09	Ferrarese *et al.* (1996)
NGC 4496A	31.02	31.13	± 0.07	Gibson *et al.* (1999)
NGC 4535	31.10	31.27	± 0.07	Macri *et al.* (1999)
NGC 4536	30.95	31.03	± 0.07	Gibson *et al.* (1999)
NGC 4548	31.04	31.24	± 0.08	Graham *et al.* (1999)
NGC 4639[d]	31.80	31.92	± 0.09	Gibson *et al.* (1999)
weighted mean	31.03	31.17	± 0.04	
		Fornax		
NGC 1326A	31.43	31.43	± 0.07	Prosser *et al.* (1999)
NGC 1365	31.39	31.50	± 0.10	Silbermann *et al.* (1999)
NGC 1425	31.81	31.93	± 0.06	Mould *et al.* (1999b)
weighted mean	31.60	31.68	± 0.14	

NOTE.— [a] Distance moduli reported by the HST Key Project on the Extragalactic Distance Scale. Random errors listed only. [b] Distance modulus corrected for metallicity using $\Delta\mu_{VI_c} = -0.24$ mag/dex (Kennicutt *et al.* 1998). [c] A full table of all Cepheid distance measurements is given in Ferrarese *et al.* (1999). [d] NGC 4639 was excluded from the determination of the mean distance to Virgo.

TABLE 3
ERROR BUDGET FOR FUNDAMENTAL PLANE AND D_n-σ

	Source	Error[a]	Notes
1. Errors in the Cepheid Distance Scale			
	A. LMC Distance Modulus	$\pm$0.13 mag	Adopted from Madore & Freedman (1999)
	B. LMC P-L zero point[b]	$\pm$0.02 mag	
S1.1	LMC P-L Systematic Error	$\pm$0.13 mag	$\sqrt{A^2+B^2}$
	C. HST V-band zero point[c]	$\pm$0.03 mag	
	D. HST I_c-band zero point[c]	$\pm$0.03 mag	
S1.2	Systematic Error in the Photometry	$\pm$0.09 mag	$\sqrt{C^2(1-R)^2+D^2R^2}$, $R \equiv A_V/E(V-I_C) = 2.47$
R1.1	Random Error in the HST Photometry	$\pm$0.05 mag	From DoPHOT/ALLFRAME comparisons
	E. Differences in R between galaxy and LMC	$\pm$0.014 mag	See Ferrarese *et al.* (1998) for details
	F. Errors in the Adopted R of LMC	$\pm$0.02 mag	See Ferrarese *et al.* (1998) for details
R1.2	Random Error in the Extinction Treatment	$\pm$0.02 mag	$\sqrt{E^2+F^2}$
	G. Typical P-L zero point Error in V	$\pm$0.05 mag	
	H. Typical P-L zero point Error in I_c	$\pm$0.04 mag	
R1.3	Typical Random Error in the Cepheid P-L zero point	$\pm$0.06 mag	
$R1_T$	Typical Random Error for an Individual Cepheid Distance[d]	$\pm$0.08 mag	$\sqrt{R1.1^2+R1.2^2+R1.3^2}$
$R1_L$	Random Error in distance to Leo I	$\pm$0.11 mag	
$R1_V$	Random Error in distance to Virgo	$\pm$0.04 mag	
$R1_F$	Random Error in distance to Fornax	$\pm$0.14 mag	
S1	Total Systematic Error in the Cepheid Distance Scale	$\pm$0.16 mag	$\sqrt{S1.1^2+S1.2^2}$
2. Errors in the Fundamental Plane and D_n-σ Relations			
	I. Observed Velocity Dispersions	$\pm$0.01 dex	
	J. Aperture Corrections	$\pm$0.01 dex	
S2.1	Systematic Error from Velocity Dispersions	$\pm$0.02 dex	$1.24 \times \sqrt{I^2+J^2}$
	K. Zero Point Error in V-band	$\pm$0.02 mag	
	L. Error in $(V-I_C)$	$\pm$0.02 mag	
	M. Transformation to Gunn r	$\pm$0.02 mag	
	N. Error Due to Color Gradients	$\pm$0.02 mag	
	O. Error in DIRBE Extinctions	$\pm$0.02 mag	
S2.2	Systematic Photometric Error in Gunn r[e]	$\pm$0.04 mag	$\sqrt{(K^2+0.4^2L^2)+M^2+N^2+O^2}$
R2.1	Random Error in measurement of $\theta_e \langle I \rangle_e^{0.82}$, r_n	$\pm$0.02 dex	
$R2.2_L$	Random Error in measurement of zero points of FP and D_n-σ for Leo I	$\pm$0.03 dex	Due to finite number of galaxies in the sample
$R2.2_V$	Random Error in measurement of zero points of FP and D_n-σ for Virgo	$\pm$0.01 dex	
$R2.2_L$	Random Error in measurement of zero points of FP and D_n-σ for Fornax	$\pm$0.03 dex	
R2.2	Internal random error in weighted mean zero point of FP and D_n-σ	$\pm$0.01 dex	Uncorrelated sum of $R2.2_L$, $R2.2_V$, and $R2.2_F$
R2.3	Random error in zero point due to random errors in the Cepheid scale	$\pm$0.01 dex	Uncorrelated sum of $R1_L$, $R1_V$, and $R1_F$
S2	Total systematic error in nearby fundamental plane and D_n-σ zero point	$\pm$0.03 dex	Uncorrelated sum of S2.1 and S2.2
R2	Total random error in nearby fundamental plane and D_n-σ zero point	$\pm$0.02 dex	Uncorrelated sum of R2.1, R2.2, and R2.3
3. Errors in the Hubble Constant			
R3.1	Random error due to peculiar velocities of distant clusters, per cluster	$\pm$1%	Estimated error is $4\%/\sqrt{N}$, where N = 11 clusters
R3.2	Random error due to uncertainties in FP and D_n-σ Slopes	$\pm$3%	
S3.1	Systematic correction due to Cepheid Metallicity Correction	$-6\% \pm 4\%$	Using $\Delta\mu_{VI_C} = -0.24$ mag/dex [O/H]
S3.2	Systematic error due to cluster population incompleteness	$\pm$2%	
S3.3	Systematic correction due to spatial coincidence of spirals and ellipticals	$-5\% \pm 5\%$	
R_{H_0}	Total Random Error in H_0	$\pm$6%	
S_{H_0}	Total Systematic Error in H_0	$\pm$11%	

NOTE.— [a] Errors are in magnitudes for Sections 1., and as indicated for Sections 2. and 3. [b] Equal to the scatter in the de-reddened PL relation for the LMC, divided by $\sqrt{N}$. [c] Contributing uncertainties from the Holtzman *et al.* (1995) zero points and the long-short uncertainty, combined in quadrature. [d] Values quoted are typical of the galaxies in the Key Project, but individual cases vary. See the individual references for the appropriate values for specific galaxies. [e] The coefficient on L is simply the color term of the transformation in §3.2.2. [f] Uncertainty in DIRBE reddening taken from Schlegel *et al.* (1998).

TABLE 4
MEAN ZERO POINTS FOR THE FUNDAMENTAL PLANE AND D_n-σ RELATIONS

Cluster	$m - M^a$ (mag)	$\langle\gamma\rangle^b$	$\langle\delta\rangle^c$	Cepheid Random (dex)	Cepheid Systematic (dex)
Leo I	$30.08 \pm 0.11 \pm 0.16$	-0.108 ± 0.033	-2.341 ± 0.033	± 0.022	± 0.032
Virgo	$31.03 \pm 0.04 \pm 0.16$	-0.182 ± 0.012	-2.403 ± 0.012	± 0.008	± 0.032
Fornax	$31.60 \pm 0.14 \pm 0.16$	-0.173 ± 0.033	-2.388 ± 0.033	± 0.028	± 0.032
weighted mean	· · ·	-0.173 ± 0.011	-2.395 ± 0.011	± 0.007	± 0.032

NOTE.— [a] Weighted mean distance moduli from Table 2 with random and systematic uncertainties. The errors in the Cepheid distance scale are detailed in Table 3
[b] $\gamma = \log r_e - 1.24 \log \sigma + 0.82 \log \langle I \rangle_e$. Internal random errors given.
[c] $\delta = \log r_n - 1.24 \log \sigma$. Internal random errors given.

TABLE 5
THE DISTANT CLUSTER SAMPLE

Cluster	N	Zero Point[a]	*rms*	D (Mpc)	$cz_{\rm CMB}$	$H_0{}^b$	$cz_{\rm flow}$	$H_0{}^b$
				Fundamental Plane				
Dorado Cluster	9	-4.336	0.103	15 ± 2	1131	78 ± 8	1064	73 ± 8
Hydra I	20	-4.886	0.141	52 ± 5	4061	79 ± 8	3881	75 ± 7
Abell S753	16	-4.892	0.098	52 ± 5	4351	83 ± 7	3973	76 ± 7
GRM 15[c]	7	-4.871	0.088	50 ± 5	4530	91 ± 9	4848	97 ± 10
Abell 3574	7	-4.908	0.095	54 ± 6	4749	87 ± 9	4617	85 ± 9
Abell 194	25	-4.942	0.093	59 ± 5	5100	87 ± 7	5208	89 ± 7
Abell S639	12	-4.970	0.087	63 ± 6	6533	104 ± 9	6577	105 ± 9
Coma Cluster	81	-5.129	0.085	90 ± 6	7143	79 ± 6	7392	82 ± 6
DC 2345-28	30	-5.205	0.079	108 ± 8	8500	79 ± 6	8708	81 ± 6
Abell 539	25	-5.204	0.068	107 ± 8	8792	82 ± 6	8648	80 ± 6
Abell 3381	14	-5.309	0.101	137 ± 12	11536	84 ± 8	11436	84 ± 8
				D_n-σ				
Dorado Cluster	9	-6.600	0.126	16 ± 2	1131	71 ± 8	1064	66 ± 8
Hydra I	20	-7.130	0.128	54 ± 5	4061	75 ± 7	3881	71 ± 7
Abell S753	16	-7.145	0.108	56 ± 5	4351	77 ± 7	3973	71 ± 6
GRM 15[c]	7	-7.092	0.086	50 ± 5	4530	91 ± 9	4848	97 ± 10
Abell 3574	7	-7.142	0.107	56 ± 6	4749	85 ± 10	4617	83 ± 9
Abell 194	25	-7.178	0.096	61 ± 5	5100	84 ± 7	5208	86 ± 7
Abell S639	12	-7.224	0.085	68 ± 6	6533	97 ± 9	6577	97 ± 9
Coma Cluster	81	-7.373	0.084	95 ± 7	7143	75 ± 5	7392	78 ± 5
DC 2345-28	30	-7.441	0.081	111 ± 8	8500	76 ± 6	8708	78 ± 6
Abell 539	25	-7.445	0.076	112 ± 8	8792	78 ± 6	8648	77 ± 6
Abell 3381	14	-7.540	0.085	140 ± 12	11536	83 ± 7	11436	82 ± 7

NOTE.— [a] These mean fundamental plane and D_n-σ zero points are given by $\gamma = \log \theta_e - 1.24 \log \sigma + 0.82 \log \langle I \rangle_e$ and $\gamma = \log \theta_n - 1.24 \log \sigma$, respectively, where θ_e and θ_n are measured in radians.
[b] The uncertainties listed are the quadrature sum of the random errors in the local, Cepheid-based zero points, the random errors in zero point for each distant cluster, and the random error due to uncertainties in the FP and D_n-σ slopes. [c] Grm 15 is the designation by Jørgensen *et al.* (1995) for southern group number 15 of Maia, da Costa, & Latham (1989).